The Journal of Energy: Engineering & Management
Vol. 10, No. 4, Winter 2021, P. 90-117

Effects of Using Sun-shape Turbulator on Thermal-Hydraulic Performances of a Heat Exchanger Filled with Nanofluid

M. Vahedi[1], Y. Mollai Barzi[2*], M. Firouzi[3]

[1] Department of Mechanical Engineering, Kashan Branch, Islamic Azad University, Kashan, I.R. Iran
Mohamad_vahedi98@yahoo.com
[2] Department of Mechanical Engineering, Kashan Branch, Islamic Azad University, Kashan, I.R. Iran
Yasermollaibarzi@gmail.com
[3] Department of physics, Kashan Branch, Islamic Azad University, Kashan, I.R. Iran
Masomeh-Firouzi@yahoo.com

Abstract

The main aim of the present article is to produce a smaller and cheaper heat exchanger with similar performance. The second goal of this investigation is to study the effects of using oil-based nano-fluids in a refinery heat exchanger. The third objective of this paper is to compare the results which are obtained from the singe- and multi-phase approaches. To fulfill this demand, ANSYS-Fluent and Aspen-HYSYS softwares are employed. Also, MgO-SAE10 nanofluid is studied in this paper using two-phase approaches. The THPEC, Thermal-Hydraulic Performance Evaluation Criteria, and specific heat flux, q'', have major roles in this paper. In the second step, the authors try to achieve an efficient model which has not only the THPEC > 1 but also the maximum value of q''. According to obtained results, the usage of nanofluid and turbulators can enhance thermal-hydraulic performances of the heat exchanger significantly. Furthermore, it is concluded that by employing nanofluid and turbulators, the cost of manufacturing refinery heat exchangers are sharply reduced. A heat exchanger filled with MgO-SAE10 nanofluid and equipped with SOL-shaped turbulators with δ=0.5mm, l=5.8mm and D=5.8mm is suggested as the best configuration, which can improve the thermal characteristics of heat exchanger about 62% in this work.

Keywords: Heat Exchangers, Sun-Shape Turbulators, Nanofluid, Two-Phase Simulation, THPEC.

❊ Corresponding Author

1. Introduction

The hot-oil-based shell and tube heat exchangers are commonly employed in order to heat crude oil in refineries. These heat exchangers increase the temperature of crude oil more than 200°C and, thus, are often so huge and expensive. Investigations on flow field and heat transfer in thermal devices for attaining better thermal efficiency is one of the plus frequent subjects in the view of technological applications. This theme has much significance from energy-saving viewpoints. Numerous tactics have been employed to attaini more efficient methods in heat exchangers. These methods have been separated into two collections: the active and the passive. In the passive collection, employing corrugations is the plus frequent procedures in improving the efficiency of heat exchangers. Refereed method causes a better mixing and breaking the laminar sub-layer and, consequently, introducing local turbulence. Introducing local turbulence leads to decreasing the thermal resistance and growing the heat transfer. Additional methods in thermal efficiency improving are employing the nanofluid. Nanofluid with better thermal conductivity may lead to more heat transfer. In current investigations, the influences of reforming geometry and employing nanofluid on flow field and heat transfer have been investigated simultaneously. It should be noted that wavy channels applications are in compact thermal devices. Therefore, the results of this study can be used in obtaining an optimum point of process of compact thermal devices.

Attributable to the significant applications of corrugated channel in thermal devices such as heat exchangers, this topic is investigated by numerous researchers. Oyakawa et al. [1] represented an investigation on a channel equipped with wavy walls. Panahi and Zamzamian [2] studied experimentally heat transfer improvement in a helical shell-and-coiled tube heat exchanger with and without turbulators. Their obtained results illustrated that the usage of helical turbulators in coiled tubes may improve the thermal efficiency of heat exchangers and obviously pressure drop. Feyza et al. [3] studied experimentally the heat transfer equipped with wire coil turbulators in a concentric tube heat exchanger filled with Al_2O_3-water nanofluid. They found that the deployment of nanofluids at low nanoparticles volume fractions does not present a significant change on the pressure drop value. Ničeno and Nobile [4] conducted a numerical investigation on turbulent forced convection fluid flow and heat transfer in a wavy channel. They reported a significant enhancement in the heat transfer after a flow regime change. Sheikholeslami and Ganji [5] studied thermal enhancement experimentally and numerically in a double pipe heat exchanger equipped with perforated turbulators. Their obtained results show that the thermal efficiency of the heat exchanger improves with an open area ratio augmentation. Also, it is realized that temperature gradient reduces with a pitch ratio augmentation. Comini et al. [6] studied thermal-hydraulic characteristics (Nusselt numbers and friction factor) of a heat exchanger equipped with turbulators. In another similar paper, Farshad and Sheikholeslami [7] investigated numerically entropy generation in a solar heat exchanger equipped with turbulators and filled with turbulent nanofluid flow. They realized that the Bejan number value declines by augmenting the friction due to an inlet velocity augmentation. Furthermore, it is found out that for higher diameter ratio values the pumping power efficacy will be more important. Liou et al. [8] studied experimentally thermal flow characteristics in a square serpentine heat exchanger equipped with louver-type turbulators. These turbulators were fitted in the twin-pass square through channel with a hydraulic diameter of 46 mm and a fully developed inlet condition. They found that the usage of turbulators increases the Nusselt number and the pressure drop penalty.

Rivier et al. [9] studied experimentally thermal improvement of a circular tube heat exchanger equipped with elliptic shaped turbulators filled with turbulent water flow. They realized that the thermal rate in a novel heat exchanger in their work increased about 900%, but there is also a very big pressure drop penalty. Jafaryar et al. [10] studied numerically the heat transfer characteristics and the entropy generation of a heat exchanger tube equipped with twisted tape turbulators filled with turbulent CuO-water nanofluid flow. Their obtained results illustrate that the improved nanofluid mixing happens for lower pitch ratio values. Also, turbulators' height has a reverse relationship with the thermal boundary layer thickness. Furthermore, it is realized that with an increase in inlet velocity, the flow develops stronger. Duan and Muzychka [11] studied analytically the thermal properties of an axial corrugated micro heat exchanger filled with laminar nanofluid flow. They realized that an in Nusselt number using turbulators also leads to an increase in the pressure drop. A numerical investigation on corrugation profile for cross-corrugated plates effect on flow field and heat transfer were conducted by Zhang and Che [12]. Reported results showed that trapezoidal channel has higher Nusselt number and friction factor than the elliptic channel. Zhang and Che [13] studied numerically thermal-hydraulic performances of a corrugated channel filled with nanofluid. They found out that the usage of wavy channels had a higher Nusselt number and a greater pressure drop compared with the results of straight channel. Santra et al. [14] studied numerically thermal efficiency of a corrugated heat exchanger filled with Cu-water nanofluid. They found out that heat transfer enhanced with employing turbulators, nanoparticles, and increasing Reynolds number. Also similar results were obtained by Abu-Nada [15] in a numerical study in a heat exchanger filled with turbulent nanofluid flow.

Xiong et al. [16] studied numerically thermal efficiency of a corrugated pipe filled with CuO-H_2O nanofluid turbulent flow employing finite volume method. They selected the single phase model for modeling the nanofluid and the k-ε to simulate the turbulence model. They realized that that usage of turbulators leads to more Nusselt numbers. Ahmadi et al. [17] studied numerically heat transfer characteristics in the case of using complex-shaped turbulators in a heat exchanger filled with nanofluid. They found that intensity of swirl flow boosts with augmenting width ratio can provide a more friction factor. Therefore, they suggested that for the improvement of energy efficiency in the pipe, employing nanofluid and turbulators are useful. Manca et al. [18] studied numerically the heat transfer and fluid flow in the ribbed channels. They found out that an upsurge in Nusselt number attended by greater friction factor due to nanoparticles volume fraction. Mohammed et al. [19] obtained numerically similar results. Heidary and Kermani [20] investigated numerically the heat transfer and fluid flow inside a heat exchanger equipped with turbulators and filled with nanofluid. They realized that Nusselt number enhanced with an increase in nanoparticles volume fraction, wave amplitude, and Reynolds number. Sheikholeslami et al. [21] studied experimentally the heat transfer characteristics of discontinuous helical turbulators of a double pipe heat exchanger filled with water and air. They found out that the Nusselt number and the friction factor reduce with an increase in the open area ratio and pitch ratio. Ahmed et al. [22] studied the thermal-hydraulic effects of a heat exchanger equipped with corrugated walls with different phase shift between the upper and lower waves. Also, Ahmed et al. [23] investigated the numerically thermal-hydraulic characteristics of a trapezoidal-corrugated channel. They found out that the usage of corrugation may lead to more heat transfer and pressure drop. In addition, phase shifts have a significant influence on theses parameters. Abbasian Arani et al. [24] and Sadripour et al. [25] studied in similar numerical investigations the thermal characteristics of corrugated heat exchangers filled with nanofluid. They found out that the thermal-hydraulic characteristics of heat exchangers are significantly influenced by varying corrugations shapes and nanoparticles morphology.

Sheikholeslami and Ganji [26] studied experimentally and numerically the heat transfer enhancement in an air-to-water heat exchanger with discontinuous helical turbulators. They realized that a higher open-area ratio offers greater thermal performance than alower one. Sandeep et al. [27] investigated the effects of novel flow divider type turbulators on the fluid flow and heat transfer. The reason why the heat transfer improves is related to the displacement of = fluid from a central core region towards the walls of tube by a novel flow divider type turbulators. Mashoofi et al. [28] studied experimentally the fabrication method and thermal-frictional behavior of a tube-in-tube helically coiled heat exchanger which contains turbulators. Yadav and Sahu [29] studied experimentally the heat transfer augmentation in a double pipe water-to-air counter flow heat exchanger with helical surface disc turbulators. The hot fluid (water) flows through the inner tube and the cold fluid (air) flows in through the annulus. The tests were conducted for air, for uniform wall temperature conditions. Nanan et al. [30] and Heris et al. [31] in similar works studied the experimentally and numerically flow and thermal mechanisms in a heat exchanger tube inserted with twisted cross-baffle turbulators. They realized that the thermal enhancement factor, friction factor, and heat transfer rate increase with the reduction of pitch ratio and an increase in the flow velocity. Mohammed et al. [32] studied a two-phase forced convection of nanofluid flow in circular tubes using convergent and divergent conical rings inserts. Four different suspensions with various nanoparticles types (ZnO, SiO_2, CuO, and Al_2O_3 with volume concentrations between 1% and 4% and particle sizes between 20nm and 50nm were analyzed. They employed two different approaches (a single-phase and a two-phase mixture) for simulating nanofluids. Karimi et al. [33] investigated the tape insert material effects on the heat transfer and flow distribution in a nanofluid-based double tube heat exchanger employing a two-phase mixture model. The effects of nanofluid and the twisted tape on the hydrodynamic and thermal performance of the heat exchanger were studied.

Sheikholeslami and Rokni [34] studied numerically the influence of melting surface on the nanofluid flow under a magnetic field by employing a two-phase model approach. The roles of the Reynolds number, Schmidt number, Brownian parameter, thermophoresis parameter, Eckert number, and melting parameter were illustrated graphically. In another similar investigation, Sheikholeslami and Rokni [35] analyzed the nanofluid flow and heat transfer in a heat exchanger under a magnetic field by employing a two-phase model. Results revealed that temperature gradient enhances with the augmentation of the suction parameter, but it reduces with the augmentation of thermophoretic parameters. Alsarraf et al. [36] studied numerically thermal-hydraulic characteristics of the turbulent boehmite alumina nanofluid flow with different nanoparticles shapes in a minichannel heat exchanger using a two-phase mixture model. In their investigation, the effects of different Reynolds numbers, nanoparticle concentrations, and morphologies were investigated. Borah et al. [37] investigated numerically the effect of non-uniform heating on a conjugate heat transfer in a duct filled with nanofluid by employing a two-phase Eulerian–Lagrangian mixture method. Barnoon et al. [38] investigated numerically the entropy generation of various nanofluid flows in an annulus in the presence of a magnetic field using single- and two-phase approaches. They realized that in all studied conditions, the predicted Nusselt number in a two-phase model is higher than calculated values in a single-phase model. Also, they found out that the maximum friction factor penalty for single- and two-phase models happens at maximum nanoparticles volume fractions and Hartman number.

It must be pointed that in the most of aforesaid numerical studies, using different ribs and corrugations has been determined to examine the influence of employing corrugated walls on the heat transfer characteristics in pipes or channels filled with base fluid or nanofluids. However, based on the above literature review, it can be observed that the influence of using turbulators in a real heat exchanger on the thermal-hydraulic performance of the forced flow filled with nanofluids has been never reported. Thus, the main goals of the present article are listed as follow:

- Investigation the thermal-hydraulic characteristics of a real heat exchanger equipped with turbulators and filled with nanofluid employing ANSYS-Fluent and Aspen-HYSYS softwares.
- Investigation the difference between the results which are obtained by employing Single- and Two-Phase models.
- Trying to achieve a smaller and cheaper heat exchanger with similar performance.

2. Material and Methods

2.1. Physical Model and Boundary Conditions

A schematic diagram of the needed process of studied refinery system is demonstrated in Fig. 1. This geometry is achieved employing Aspen-HYSYS software for interested process which should increases the crude oil temperature with 17,050 kg/h mass flow rate from 30°C to 240°C using pure SAE10 oil as cooling fluid. Since the specific heat capacity of crude oil depends very much on temperature and since the crude oil temperature increases in refineries, multi-steps heat exchangers are always employed. In Fig. 1 a two-step heat exchanger is shown. As it is seen in this figure, the heat exchanger number one increases the crude oil temperature from 30°C to 195°C (ΔT=165°C), and the heat exchanger number two increases the crude oil temperature from 195°C to 240°C (ΔT=45°C). It is while the geometry of both heat exchangers is similar and the reason for such behavior is related to higher specific heat capacity of crude oil at higher temperatures [39]. The thermophysical properties of crude oil are calculated using bellow equations [39]:

$$\rho_{cro}(T) = -0.735T + 1070 \quad (1)$$

$$c_{p,cro}(T) = 4.348T + 635.2 \quad (2)$$

$$\mu_{cro}(T) = 10^{-5}T^2 - 0.007T + 1.163 \quad (3)$$

$$k_{cro}(T) = -2.3 \cdot 10^{-5}T + 0.21417 \quad (4)$$

where ρ_{cro}, $c_{p,cro}$, μ_{cro} and k_{cro} are density, specific heat capacity, dynamic viscosity, and thermal conductivity of crude oil at T temperature respectively. Fig. 2 shows the schematic diagram of heat exchanger cross section (tube sides) which is achieved employing Aspen-HYSYS and Solid Works softwares for the interested process.

For investigating the effects of using turbulators or nanofluids in a heat exchanger in ANSYS-Fluent software, just one tube part with an outer area of 1 m^2 is investigated. Fig. 3 illustrates the schematic diagram of a studied geometry in ANSYS-Fluent software and the grid mesh layout. The geometry is made from two three-dimensional concentric tubes with a diameter of $\emptyset$=19.05mm and J=40.00 mm respectively. The inner tube is one part of tube section of the heat exchanger and is made of SS 304 steel with a tube thickness of 1.25 mm and the outer tube is the space to simulate the shell side of the heat exchanger. The major parameter is $q''=Q/A$ to investigate the usage of different turbulators and nanofluids; Q is the heat flux on the outer surface of inner tube and A=10 mm^2. Fig. 4 depicts the different levels of the flowchart of the present study. As it is seen in this figure, the present work is done using ANSYS-Fluent and Aspen-HYSYS softwares. The simulated configuration consists of three sections: the inlet section, the test section, and the outlet section. The test section length is L_2=60.67 mm, accompanied with the inlet section length of L_1=140 mm to guarantee a fully developed flow in the test section. In addition, an outlet section with the length of L_3=30 mm is used in order to avoid the adverse pressure effects on fluid or nanofluid flow and heat transfer characteristics in the computational domain. Fig. 5 demonstrates the schematic diagram of the studied turbulators in the present study. One of the main aims of the present study is to select the most efficient turbulators for the studied heat exchanger using thermal-hydraulic analysis. The investigated turbulators in this study are solar-corrugated (SOL) models. The different geometrical parameters of this model will be analyze in this paper using fillet, deploying different fin lengths, and employing holes on the fins.

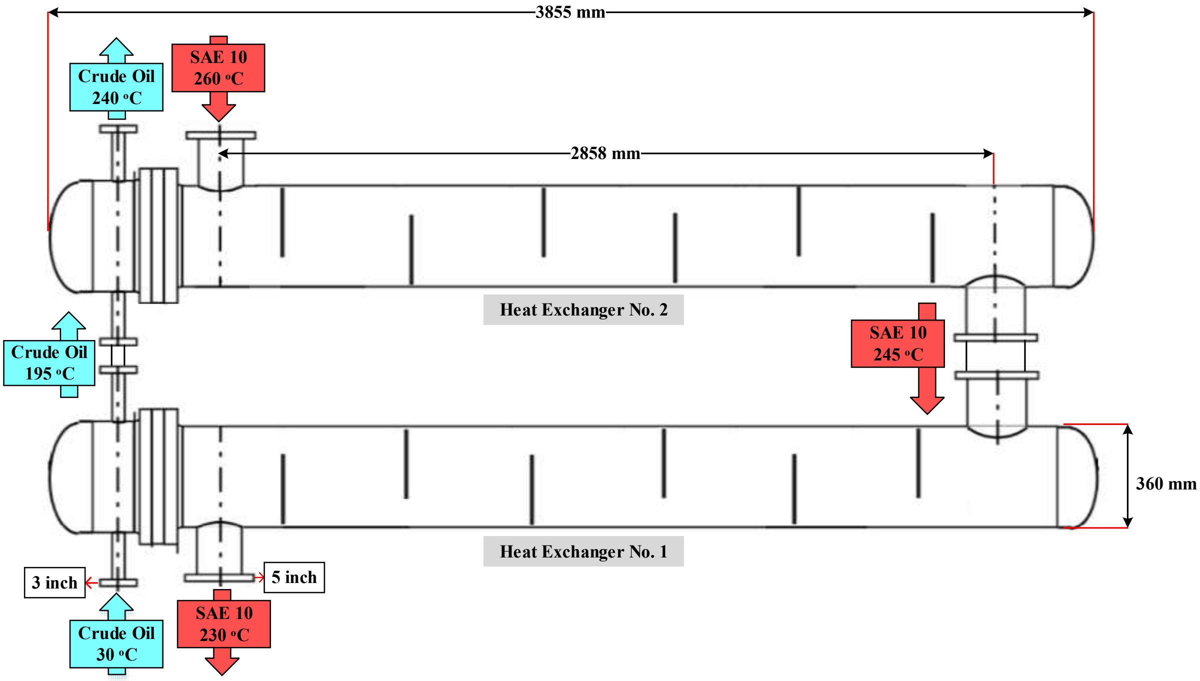

Fig. 1: Schematic diagram of the needed process for studied refinery system which is achieved employing Aspen-HYSYS software for interested process

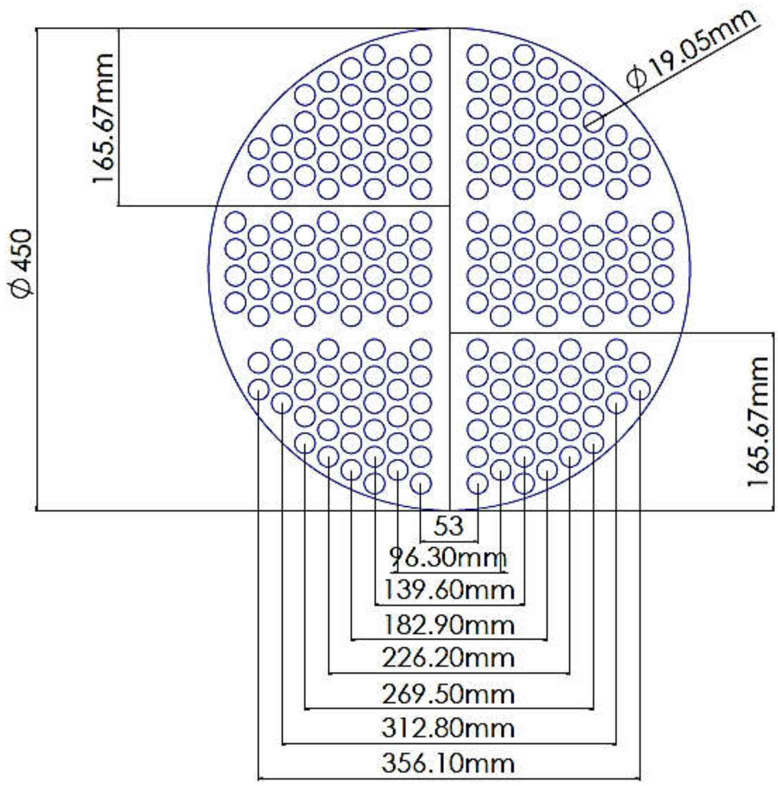

Fig. 2: Schematic diagram of heat exchanger cross section (tube sides) which is achieved employing Aspen-HYSYS and SolidWorks softwares for interested process

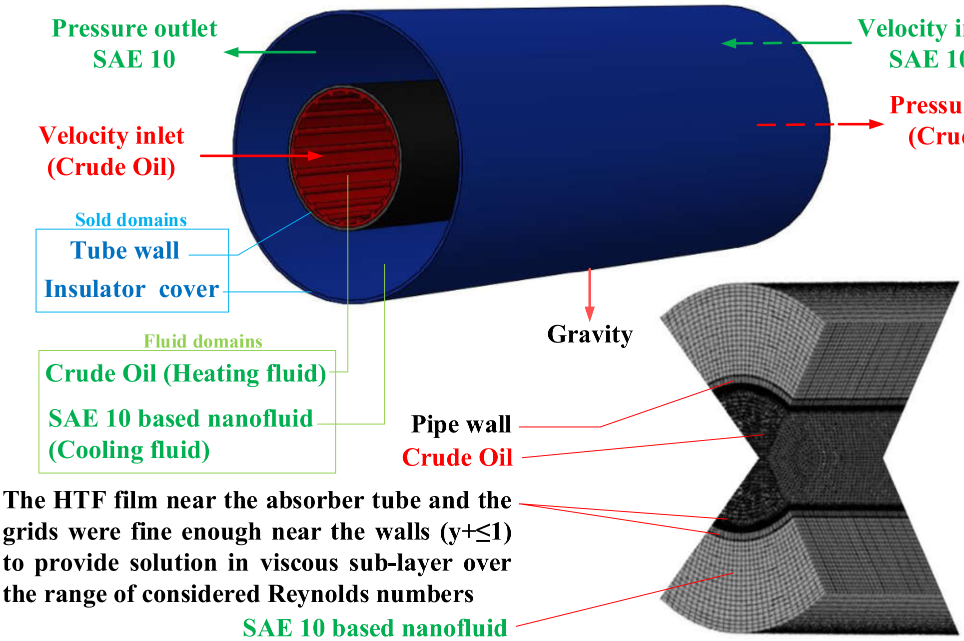

Fig. 3: Schematic diagram of studied geometry in ANSYS-Fluent software and grid mesh layout

The second aim of this investigation is to study the effects of using oil-based nanofluids in a refinery heat exchanger. For fulfilling this demand, MgO-SAE10 nanofluid is studied in this paper using a two-phase approach.

The third goal of this paper is to compare the results which are obtained from the single- and multi-phase approaches. The governing equations have been solved according to the *Eulerian-Eulerian* single fluid *Two-Phase Models* (TPM), with presumptions that the coupling between phases is strong, and the nanoparticles follow the suspension flow carefully [40]. The two phases (fluid and solid) have been determined to be inter-penetrating; it means that each fluid or solid phase has its own velocity field, and within any control volume there is a volume concentration of the first phase (base fluid) and another volume concentration for the second phase (solid nanoparticles).

To calculate the thermophysical properties of the nanofluid by using Brownian motion of nanoparticles--, the following relations are obtained [41-45]:

Density:

$$\rho_{nf} = (1-\varphi)\rho_{bf} + \varphi\rho_p \quad (5)$$

Heat capacity:

$$c_{p,nf} = (1-\varphi)c_{p,bf} + \varphi c_{p,p} \quad (6)$$

For low temperature thermophysical properties of MgO-SAE10 nanofluids in case of dynamic viscosity and thermal conductivity versus temperature are reported by Asadi and Pourfattah [39] based on experimental data at temperature T for particle concentration of φ using bellow equations:

Dynamic viscosity:

$$\mu_{nf}(T) = A + B\varphi \quad (7)$$

Thermal conductivity:

$$k_{nf}(T) = C + D\varphi \quad (8)$$

where ρ_{nf}, ρ_p and ρ_{bf} are density of nanofluid, nanoparticles and the base fluid respectively. Also $c_{p,nf}$, $c_{p,p}$ and $c_{p,bf}$ are the density of the nanofluid, nanoparticles, and the base fluid respectively. Furthermore, μ_{nf} and k_{nf} are the dynamic viscosity and thermal conductivity of nanofluid.

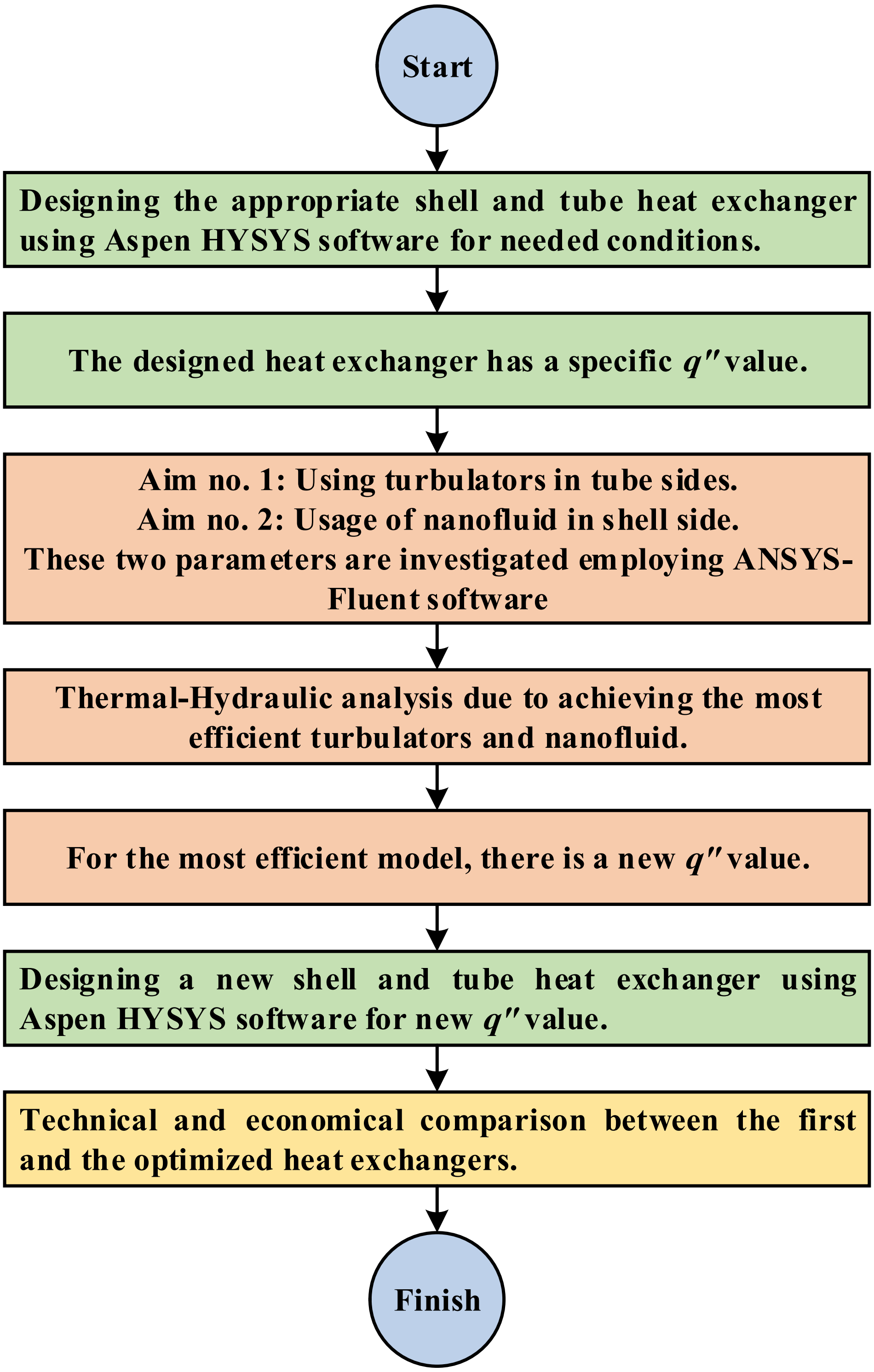

Fig. 4: Flowchart of different levels in present study

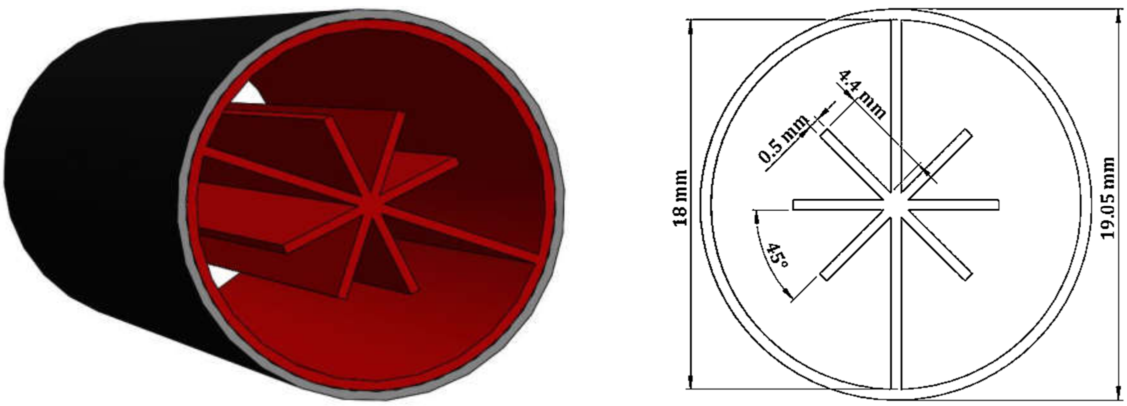

(a) Schematic diagram of complete tube and mechanical drawing

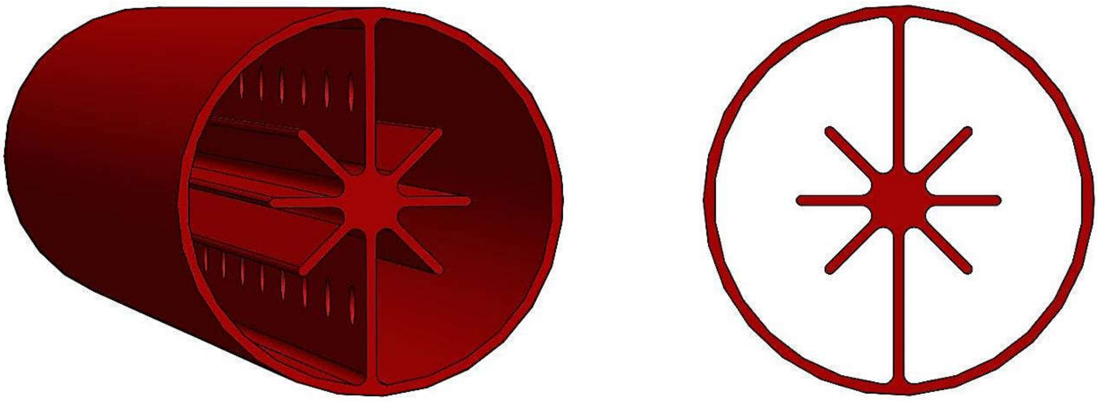

(b) The solar tabulator system

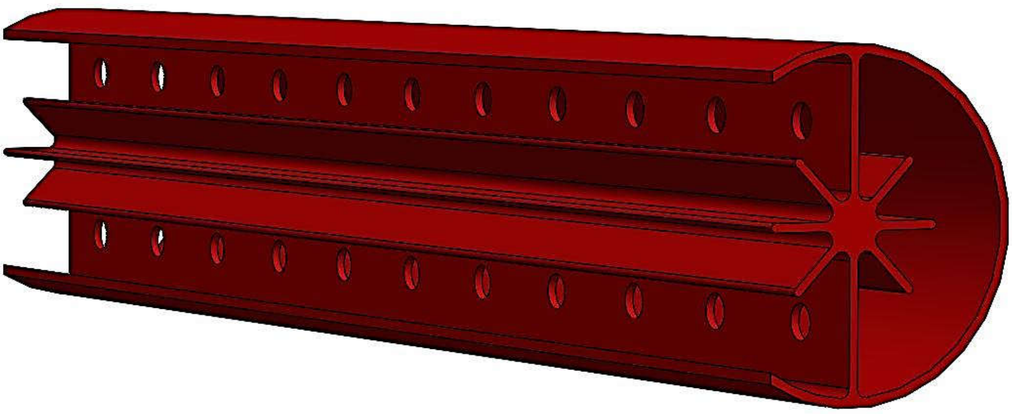

(c) The catted-view of solar tabulator system

(d) Side view of solar tabulator system

Fig. 5: Schematic diagram and plane of studied turbulators in presents study for solar-corrugated (SOL) model: (a) common model, (b) model with fillet and holes on fins, (c) cropped view, (d) holes on fins

Table 1 reports the essential coefficients to calculate Eq. (7) and Table 2 presents needed coefficients for calculating Eq. (8). Also Table 3 reports thermophysical properties of the studied nanoparticles [39]. Fig. 6 and Fig. 7 show low temperature thermophysical properties of MgO-SAE10 nanofluids in case of dynamic viscosity thermal conductivity versus particles rotational speed, nanoparticles volume fraction and temperature.

In order to calculate the thermophysical properties of oil-based nanofluid at middle temperatures following equations are reported [46]:

Thermal conductivity:

$$\frac{k_{nf}}{k_f} = 1 + 4.4Re_{np}^{0.4}Pr^{0.66}\left(\frac{T}{T_{fr}}\right)^{10}\left(\frac{k_{np}}{k_{bf}}\right)^{0.03}\varphi^{0.66} \tag{9}$$

where Re_{np} is the Reynolds number of nanoparticle, Pr is non-Newtonian base fluid Prandtl number; T is temperature of non-Newtonian nanofluid; T_{fr} is non-Newtonian base fluid freezing point; k_{np} is thermal conductivity of nanoparticles; and φ is suspended nanoparticles volume concentration. In more detail, the nanoparticle Reynolds number is defined as [46]:

$$\mathrm{Re}_{np} = \frac{\rho_{bf}\, u_B d_{np}}{\mu_{bf}} \tag{10}$$

Table 1: Coefficients for Eq. (3)[39]

Temperature (°C)	*A*	*B*	*C*	*D*
15	269.85	2110.65	0.1435	0.8526
25	165.17	1387.78	0.1453	1.0026
35	106.85	971.49	0.1462	1.1928
45	71.69	657.72	0.1479	1.2522
> 55	50.27	444.55	0.1489	1.4050

Table 2: Coefficients for Eq. (4)[39]

Temperature (°C)	*A*	*B*	*C*	*D*
15	247.72	1200.95	0.1519	0.9090
25	143.57	738.20	0.1532	0.8670
35	80.59	1265.62	0.1551	0.8580
45	52.52	636.16	0.1552	1.0007
> 55	33.58	610.77	0.1561	1.0500

Table 3: Thermophysical properties of studied nanoparticles [39]

Characteristic	MgO
Purity	99 + %
Size (nm)	40
Specific surface area (SSA) (m^2/g)	> 60
True Density (ρ) (g/m^3)	3.58
Thermal Conductivity (W/m·K)	4.9
Specific heat capacity (c_p) (kJ/kg·K)	0.937

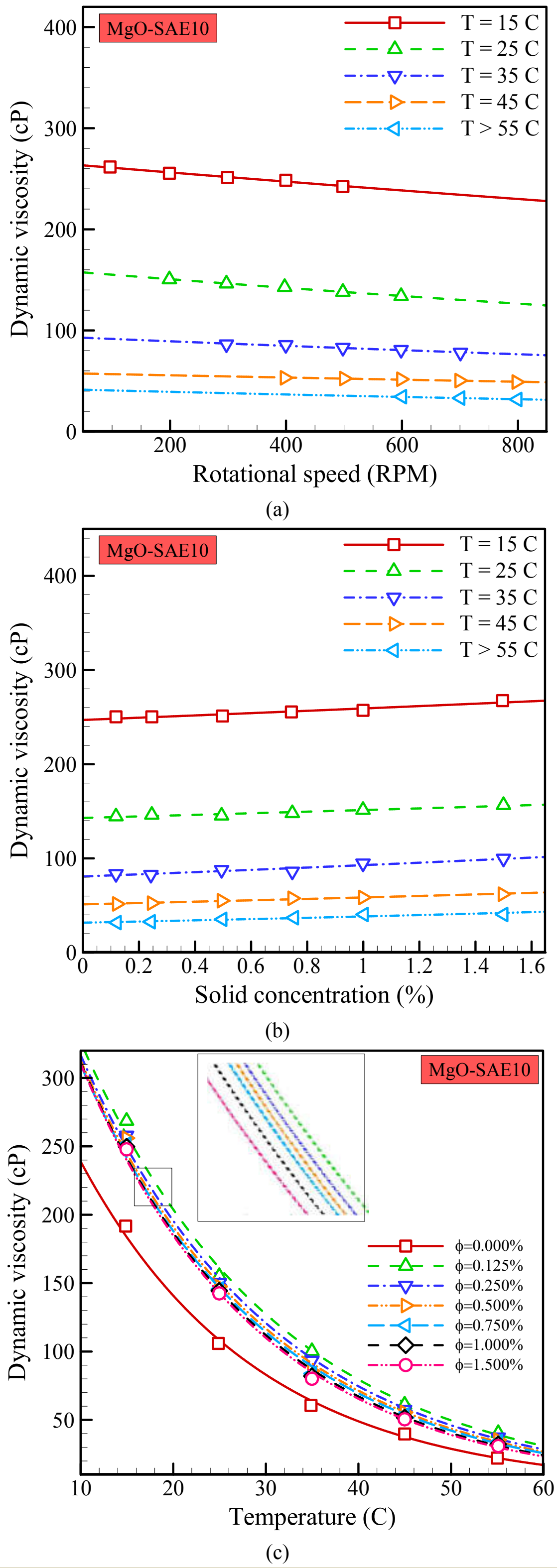

Fig. 6: Low temperature thermophysical properties ofMgO-SAE10 nanofluid in case of (a) dynamic viscosity versus particles rotational speed, (b) dynamic viscosity versus nanoparticles volume fraction and (c) dynamic viscosity versus temperature [39]

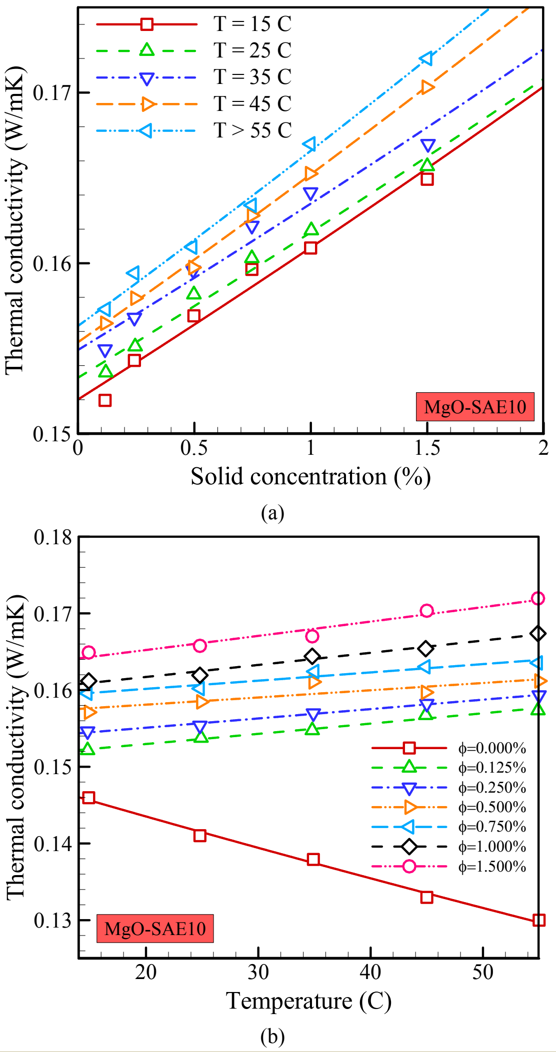

Fig. 7: Low temperature thermophysical properties of MgO-SAE10 nanofluid in case of (a) thermal conductivity versus nanoparticles volume fraction and (b) thermal conductivity versus temperature [39]

where ρ_f, μ_f, $u_{B,}$ and d_{np} are non-Newtonian base fluid density and dynamic viscosity, mean nanoparticle Brownian velocity, and the nanoparticles diameter respectively. Assuming that agglomeration is neglectable, the nanoparticles' Brownian velocity u_B has been achieved as the ratio between the time τ_d required to cover such distance and nanoparticles diameter d_{np}, which with the equation of Keblinski et al. [47] is presented as:

$$\tau_d = \frac{{d_{np}}^2}{6D_B} \tag{11}$$

where D_B is the Brownian diffusion coefficient has been assumed using the equation of Einstein-Stoke [46]:

$$D_B = \frac{k_b T}{3\pi \mu_f d_{np}} \tag{12}$$

where k_b is the Boltzmann constant is about $1.38066 \cdot 10^{-23}$ J/K. Hence [46]:

$$u_B = \frac{2k_b T}{\pi \mu_f {d_{np}}^2} \tag{13}$$

By replacing Eq. (13) in Eq. (10), we obtain [46]:

$$\mathrm{Re}_{np} = \frac{2\rho_f k_b T}{\pi {\mu_f}^2 d_{np}} \tag{14}$$

Dynamic viscosity [46]:

$$\frac{\mu_{nf}}{\mu_f} = \left(1 - 34.87\left(\frac{d_{np}}{d_f}\right)^{-0.3} \varphi^{1.03}\right)^{-1} \tag{15}$$

In the above equation d_f is non-Newtonian base fluid molecule equivalent diameter at the reference temperature T_0=293K on the basis relation $M = \rho f_0 \forall m N$, where M, ρ_{f0} and $\forall m$ are the molar mass, density at T_0 temperature and non-Newtonian base fluid molecular volume, whilst $N = 6.022 \cdot 10^{23}$ (mol^{-1}) is the Avogadro number. Also, $\forall m$ is assumed as $(4/3)\pi(df/2)^3$ and finally the equation is expressed as [46]:

$$d_f = 0.1\left(\frac{6M}{N\pi\rho_{f0}}\right)^{1/3} \tag{16}$$

Thermal diffusivity:

$$\alpha_{nf} = \frac{k_{nf}}{(\rho c_p)_{nf}} \tag{17}$$

The FVM or finite volume method has been applied in the current work. Also, in all numerical simulations of this work, the velocity-pressure coupled equations are applied. For attaining a significant accuracy in numerical problem, SIMPLEC algorithm is employed (the second order discretization). For all studied configurations and in the range of all studied Reynolds numbers and nanopaticles volume fractions, to use less CPU space on the computer, and also to economize numerical solution process, the most 10^{-6} error remainder is adopted. Also, standard k-ε turbulence model with thermal effects and pressure gradient with enhanced wall function is used in a numerical method [24, 25, 41, 42].

2.2. Governing Equations

The governing equation system for a two-phase heat transfer and nanofluid flow in the heat exchanger is written as [40, 48, 49]:

Continuity equation:

$$\nabla \cdot (\rho_{nf} V_m) = 0 \tag{18}$$

where V_m is the mean velocity andρ_{nf} is the nanofluid density.

Momentum equation:

$$\nabla \cdot (\rho_{nf} V_m V_m) = -\nabla P + \nabla \cdot (\mu_{nf} \nabla V_m) + (M \cdot \nabla) \cdot B \tag{19}$$

where μ_{nf} is the viscosity of nanofluid.

Energy equation (M=H=0):

$$\nabla \cdot (\rho_{nf}\, c\, V_m\, T) = \nabla \cdot (K_{nf}\, \nabla\, T) + \mu_0 (M \cdot \nabla) \cdot H \tag{20}$$

To analyze and to compare the heat transfer and fluid flow characteristics of various turbulator configurations in the tubes, some definitions are given as [41-45]:

The Reynolds number is defined as:

$$Re = \frac{\rho_{nf} V_m D_h}{\mu_{nf}} \tag{21}$$

where $V_m$is the mean velocity of fluid over the cross section.

The average Nusselt number is defined as [41-45]:

$$Nu_{av} = \frac{h D_h}{k_{nf}} \tag{22}$$

where h and $k_{nf}$are the average heat transfer coefficient and the thermal conductivity of nanofluid respectively.

The pressure reduction between the inlet and the outlet is demarcated as follows [41-45]:

$$\Delta p = p_{av,inlet} - p_{av,outlet} \tag{23}$$

The average friction factor of a fully developed nanofluid flow is as follows [41-45]:

$$f = \frac{2}{\left(\frac{L}{D_h}\right)} \frac{\Delta p}{\rho_{nf} {V_m}^2} \tag{24}$$

The THPEC or Thermal-Hydraulic Performance Evaluation Criteria index is defined in order to compute the thermal and fluid-dynamic performances of the tubes with different turbulator geometries to gain heat transfer enhancement seeing upsurge power pumping. It is assessed by the usage of the predicted friction factor and predicted Nusselt numbers from the fluid flow and the heat transfer field as follows [41-45]:

$$THPEC = \left(\frac{Nu_{av}}{Nu_{av,s}}\right) \cdot \left(\frac{f}{f_s}\right)^{-1/3} \tag{25}$$

Where Nu_{av} and $Nu_{av,s}$ are theestimated averaged Nusselt number for a tube with turbulators and a smooth pipe respectively. Also, f and f_s are the friction factors for a tube with turbulators and a smooth pipe respectively.

2.3. Model Validation

As shown in Table 7, a grid independence test was performed for a conventional collector using water to analyze the effects of grid sizes on the results. As it is seen, six sets of mesh are generated and tested. By comparing the results, it is concluded that mesh configurations contain a grid number of 2,933,289 nodes which is assumed to enjoy a satisfactory agreement between the computational time and the accuracy of the results with a maximum error of 0.03 percent.

Table 7: Grid independence test for sheet and tube collector

No.	Nodes	Nu	Error (%)
1	462,727	84.4579	15.51
2	856,009	71.3579	6.27
3	1,365,347	66.8734	9.27
4	2,124,817	60.6703	3.96
5	2,721,873	58.2745	0.03
6	2,933,289	58.2567	–

The Computational Fluid Dynamics (CFD) code validation was done by the comparison of numerical and experimental results obtained from previous investigations with the obtained results from the present study. Fig. 8 shows the comparison of the present results with the the experimental results of Kim et al. [50] and numerical results of Karimi et al. [33] in case of the heat transfer coefficient versus Reynolds number for a tube filled with pure water and The pressure reduction between the inlet and the outlet is demarcated as follows fluid. Also, Fig. 9 illustrates the comparison of the present results with the previous researches [32, 51, 52] in case of average Nusselt number versus Reynolds number for a tube filled with pure water and The pressure reduction between the inlet and the outlet is demarcated as follows fluid. It can be seen from these figures that there is remarkable agreement between the previous numerical and experimental results and the numerical data achieved from this paper.

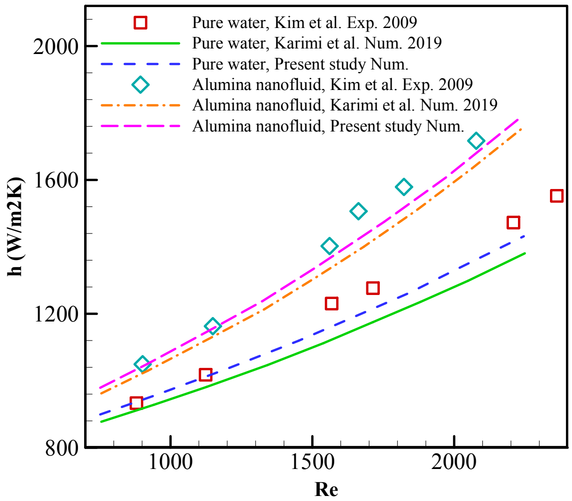

Fig. 8: Comparison of the present results with the experimental results of Kim et al. [50]and numerical results of Karimi et al. [33]in case of heat transfer coefficient versus Reynolds number for tube filled with pure water and nanofluid

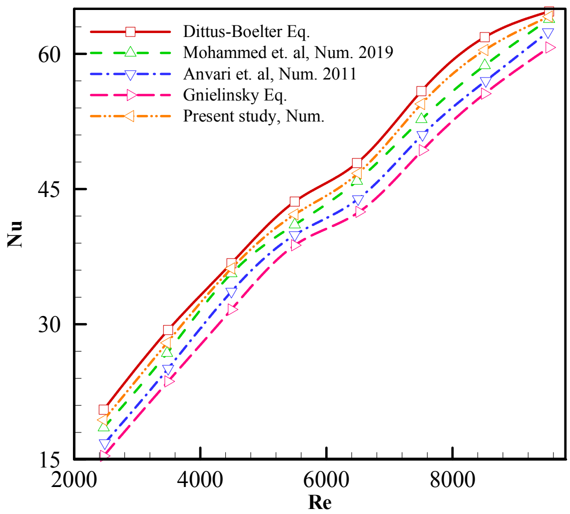

Fig. 9Comparison of the present results with the previous researches [32, 51, 52] in case of average Nusselt number versus Reynolds number for tube filled with pure water and nanofluid

3. Results and Discussion

As it is shown in Fig. 4, this investigation has been done in three steps:

1. Designing a heat exchanger employing Aspen-HYSYS software according to the demands reported in Fig. 1.

2. The consumption of a section of a heat exchanger with pipe-surface- is of 10 mm^{2,} and analyzing this domain in order to investigate the thermal-hydraulic performances of the studied section in case of using The pressure reduction between the inlet and the outlet is demarcated as follows fluid and turbulators employing ANSYS-Fluent 15.0 software.

3. The Thermal-Hydraulic Performance Evaluation Criteria (THPEC) and specific heat flux (q'') have major roles in this paper. In the second step, the authors try to achieve an efficient model which has not only the THPEC > 1, but also a maximum value of q''. For this efficient model and according to its q'', one more time a real heat exchanger is designed employing Aspen-HYSYS 10.0 software.

3.1. Step Number One

As it is noted previously, the demanded heat exchanger in this paper should increases the crude oil temperature with 17,050 kg/h mass flow rate from 30°C 240°C using pure SAE10 oil as cooling fluid. Since the specific heat capacity of crude oil depends very much on temperature, and since crude oil temperature increases in refineries, a two-step heat exchanger is designed in this paper (see Fig. 1). It should be noted that the geometries of the both heat exchangers are similar with each other. Table 8 and Table 9 report the specification sheets of Heat Exchanger 1 and 2 respectively. The specific heat fluxes of these heat exchangers are q''=56.51 W/m^2 and q''=18.64 W/m^2 respectively. These heat exchangers are filled with SAE10 and crude oil as cooling and heating fluids respectively. In the second step, the usage of The pressure reduction between the inlet and the outlet is demarcated as follows fluid and turbulators are analyzed to achieve the most q'' value considering THPEC value.

3.2. Step Number Two

3.2.1. Usage of Nanofluid

Fig. 10 illustrates the comparison of results of different phase models simulations in case of average Nusselt number, friction factor, THPEC, and specific heat transfer, with different nanopaticles volume concentrations for Heat Exchanger number 1 filled with MgO-SAE10 The pressure reduction between the inlet and the outlet is demarcated as follows fluid. It is seen that the usage of TPM leads to more Nusselt number, friction factor, THPEC, and specific heat transfer than using SPM, in all ranges of nanopaticles volume fractions. Fig. 10a shows the comparison of results of different phase models simulations in case of average Nusselt number versus different nanoparticles volume concentrations for Heat Exchanger number 1 filled with MgO-SAE10 nanofluid. It is realized that the usage of nano-fluid significantly increase the Nusselt number values and at φ=1.5% the Nusselt number value increases about 174% and 190% than the base fluid for SPM and TPM respectively. Fig. 10b shows the comparison of results of different phase model simulations in case of average friction factor with different nanopaticles volume concentrations for Heat Exchanger number 1 filled with MgO-SAE10 The pressure reduction between the inlet and the outlet is demarcated as follows fluid.

It is realized that the usage of nano-fluid significantly increases the average friction factor values, and at φ=1.5% the average friction factor value increases about 200% and 218% than the base fluid for SPM and TPM respectively. Fig. 10c shows the comparison of the results ofdifferent phase model simulations in case of THPEC with different nanopaticles volume concentrations for Heat Exchanger number 1 filled with MgO-SAE10 The pressure reduction between the inlet and the outlet is demarcated as follows fluid. It is seen that the usage The pressure reduction between the inlet and the outlet is demarcated as follows fluid at all range of nanopaticles volume fractions is efficient according to the thermal-hydraulic viewpoint. Also, it is realized that the usage of The pressure reduction between the inlet and the outlet is demarcated as follows fluid significantly increases the THPEC values, and at φ=1.5% the THPEC value increases about 90% and 97% than the base fluid for SPM and TPM respectively. Fig. 10d shows the comparison of the results of different phase model simulations in case of specific heat transfer with different nanoparticles volume concentrations for Heat Exchanger number 1 filled with MgO-SAE10 nanofluid. It is realized that the usage of nanofluid significantly increases the specific heat transfer values sand at φ=1.5% the specific heat transfer value increases about 32% and 40% than the base fluid for SPM and TPM, respectively.

Fig. 11 illustrates the comparison of the results of different phase model simulations in case of average Nusselt number, friction factor, THPEC and, specific heat transfer, with different nanopaticles volume concentrations for Heat Exchanger number 2 filled with MgO-SAE10 nanofluid. It is seen that the usage of TPM leads to a higher Nusselt number, friction factor, THPEC, and specific heat transfer than using SPM in all ranges of nanoparticles volume fractions. Fig. 11a shows the comparison of results of different phase model simulations in case of average Nusselt number with different nanopaticles volume concentrations for Heat Exchanger number 2 filled with MgO-SAE10 The pressure reduction between the inlet and the outlet is demarcated as follows fluid. It is realized that the usage of nanofluid significantly increases the Nusselt number values, and at φ=1.5% the Nusselt number value increases about 173% and 189% than the base fluid for SPM and TPM respectively. Fig. 11b shows the comparison of results of different phase model simulations in case of average friction factor with different nanopaticles volume concentrations for Hheat exchanger number 2 filled with MgO-SAE10 The pressure reduction between the inlet and the outlet is demarcated as follows fluid. It is realized that the usage of The pressure reduction between the inlet and the outlet is demarcated as follows fluid significantly increases the average friction factor values, and at φ=1.5% the average friction factor value increases about 199% and 218% than base fluid for SPM and TPM respectively. Fig. 11c shows the comparison of results of different phase model simulations in case of THPEC with different nanopaticles volume concentrations for heat exchanger number 2 filled with MgO-SAE10 The pressure reduction between the inlet and the outlet is demarcated as follows fluid. It is seen that the usage of nanofluid at all ranges of nanopaticles volume fractions is efficient according to the thermal-hydraulic viewpoint. Also, it is found out that the usage of nanofluid significantly increases the THPEC values, and at φ=1.5% the THPEC value increases about 89% and 96% than the base fluid for SPM and TPM respectively. Fig. 11d shows the comparison of results of different phase model simulations in case of specific heat transfer with different nanoparticles volume concentrations for Heat Exchanger number 2 filled with MgO-SAE10 The pressure reduction between the inlet and the outlet is demarcated as follows fluid. It is realized that the usage of nanofluid significantly increases the specific heat transfer values, and at φ=1.5% the specific heat transfer value increases about 32% and 40% than the base fluid for SPM and TPM respectively.

Table 8: Heat Exchanger number 1 specification sheet

Paper: Two-phase simulation of nanofluid flow in a heat exchanger equipped with vortex generator							
Location: Iran							
Service of Unit:	Our Reference:						
Item No.: 1 with Base Fluid	Your Reference:						
Date:	Rev No.:	Job No.:					
Size	457 - 3000 mm	Type	BEU Hor	Connected in	1 parallel	1 series	
Surf/unit(eff.)	40.1 m²	Shells/unit	1	Surf/shell (eff.)	40.1 m²		
PERFORMANCE OF ONE UNIT							
Fluid allocation		**Shell Side**		**Tube Side**			
Fluid Name		SAE 10		Crude oil			
Fluid quantity, Total	kg/h	188852		17050			
Vapor (In/Out)	kg/s	0	0	0	0		
Liquid	kg/s	52.4589	52.4589	4.7361	4.7361		
Noncondensable	kg/s	0		0			
Temperature (In/Out)	°C	245	231.22	30	180.35		
Dew / Bubble point	°C						
Density (Vap / Liq)	kg/m³	/ 859.33	/ 859.33	/ 863.53	/ 765.03		
Viscosity	mPa-s	/ 0.2489	/ 0.3103	/ 8.0873	/ 0.7918		
Molecular wt, Vap							
Molecular wt, NC							
Specific heat	kJ/(kg-K)	/ 2.192	/ 2.192	/ 1.914	/ 2.535		
Thermal conductivity	W/(m-K)	/ 0.1174	/ 0.1174	/ 0.1316	/ 0.1208		
Latent heat	kJ/kg						
Pressure (abs)	bar	10	9.85323	16	15.87748		
Velocity (Mean/Max)	m/s	1.2 /	2.38	0.75 /	0.85		
Pressure drop, allow./calc.	bar	1	0.14677	1	0.12252		
Fouling resistance (min)	m²-K/W	0.00025		0.00025	0.00029	Ao based	
Heat exchanged	2266	kW		MTD corrected	113.7	°C	
Transfer rate, Service	347.5	Dirty	347.5	Clean	427.4	W/(m²-K)	
CONSTRUCTION OF ONE SHELL				**Sketch**			
		Shell Side	**Tube Side**				
Design/vac/test pressure:g	bar	11.032 / /	17.93 / /				
Design temperature	°C	282.22	282.22				
Number passes per shell		1	6				
Corrosion allowance	mm	3.18	0				
Connections In	mm	1 254 / -	1 50.8 / -				
Size/rating Out		1 203 / -	1 76.2 / -				
Nominal Intermediate		/ -	/ -				
Tube No.	108*2=216	OD 19.05	Tks- Avg 1.25 mm	Length 3000 mm	Pitch	23.81 mm	
Tubetype	Plain	#/m	Material	SS 304	Tube pattern	30	
Shell	Carbon Steel	ID 450	OD 469.05 mm	Shell cover	Carbon Steel		
Channel or bonnet		Carbon Steel		Channel cover	-		
Tubesheet-stationary		Carbon Steel		Tubesheet-floating	-		
Floating head cover		-		Impingement protection	None		
Baffle-cross	Carbon Steel	Type	Single segme Cut(%d)	47 H	Spacing: c/c	420 mm	
Baffle-long	-	Seal type			Inlet	0 mm	
Supportstube		UBend	0	Type			
Bypass seal		Tube-tubesheet joint		Exp. 2 grv			
Expansion joint	-	Type	None				
RhoV2-Inlet nozzle	1237	Bundle entrance	5481	Bundle exit	343	kg/(m-s²)	
Gaskets - Shell side	Flat Metal Jacket Fibe	Tube Side	Flat Metal Jacket Fibe				
Floating head	-						
Code requirements	ASME Code Sec VIII Div 1		TEMA class	R - refinery service			
Weight/Shell	1075.4	Filled with water	1529.2	Bundle	475.8	kg	
Remarks							
q" = 56.51 kW/m2							

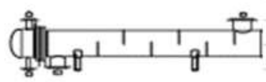

Table 9: Heat Exchanger number 2 specification sheet

Company: Two-phase simulation of nanofluid flow in a heat exchanger equipped with vortex generator												
Location: Iran												
Service of Unit: 2 with Base Fluid	Our Reference:											
Item No.:	Your Reference:											
Date:	Rev No.:	Job No.:										
Size	457	-	3000	mm	Type	BEU	Hor	Connected in	1	parallel	1	series
Surf/unit(eff.)	40.1	m²	Shells/unit	1	Surf/shell (eff.)	40.1	m²					
PERFORMANCE OF ONE UNIT												
Fluid allocation		**Shell Side**		**Tube Side**								
FluidName		SAE 10		Crude oil								
Fluid quantity, Total	kg/h	188852		17050								
Vapor (In/Out)	kg/s	0	0	0	0							
Liquid	kg/s	52.4589	52.4589	4.7361	4.7361							
Noncondensable	kg/s	0		0								
Temperature (In/Out)	°C	260	253.5	180	240.71							
Dew / Bubble point	C											
Density (Vap / Liq)	kg/m³	/ 859.33	/ 859.33	/ 765.26	/ 752.9							
Viscosity	mPa-s	/ 0.1963	/ 0.2175	/ 0.7954	/ 0.4482							
Molecular wt, Vap												
Molecular wt, NC												
Specific heat	kJ/(kg-K)	/ 2.192	/ 2.192	/ 2.534	/ 2.612							
Thermal conductivity	W/(m-K)	/ 0.1174	/ 0.1174	/ 0.1208	/ 0.1194							
Latent heat	kJ/kg											
Pressure (abs)	bar	10	9.85991	16	15.87693							
Velocity (Mean/Max)	m/s	1.2 /	2.38	0.81 /	0.87							
Pressure drop, allow./calc.	bar	1	0.14009	1	0.12307							
Fouling resistance (min)	m²-K/W	0.00025		0.00045	0.00052	Ao based						
Heat exchanged	747.2	kW	MTD corrected	38.53	°C							
Transfer rate, Service	483.7	Dirty	483.8	Clean	769.8	W/(m²-K)						
CONSTRUCTION OF ONE SHELL					**Sketch**							
		Shell Side		**Tube Side**								
Design/vac/test pressure:g	bar	11.032 / /		17.93 / /								
Design temperature	°C	298.89		298.89								
Number passes per shell		1		6								
Corrosion allowance	mm	3.18		0								
Connections	In	mm	1	254	/	-	1	50.8	/	-		
Size/rating	Out		1	203	/	-	1	76.2	/	-		
Nominal	Intermediate				/	-			/	-		
Tube No.	108*2=216	OD	19.05	Tks-	Avg	1.25	mm	Lengtl 3000	mm	Pitch	23.81	mm
Tubetype	Plain	#/m	Material	SS 304	Tube pattern	30						
Shell	Carbon Steel	ID	450	OD 469.05	mm	Shell cover	Carbon Steel					
Channel or bonnet	Carbon Steel	Channel cover	-									
Tubesheet-stationary	Carbon Steel	Tubesheet-floating	-									
Floating head cover	-	Impingement protection	None									
Baffle-cross	Carbon Steel	Type	Single segme Cut(%d)	47	H	Spacing: c/c	420	mm				
Baffle-long	-	Seal type	Inlet	0	mm							
Supportstube	UBend	0	Type									
Bypass seal	Tube-tubesheet joint	Exp. 2 grv										
Expansion joint	-	Type	None									
RhoV2-Inlet nozzle	1237	Bundle entrance	5481	Bundle exit	343	kg/(m-s²)						
Gaskets - Shell side	Flat Metal Jacket Fibe	Tube Side	Flat Metal Jacket Fibe									
Floating head	-											
Code requirements	ASME Code Sec VIII Div 1	TEMA class	R - refinery service									
Weight/Shell	1075.4	Filled with water	1529.3	Bundle	475.8	kg						
Remarks												
q"=18.64 kW/m2												

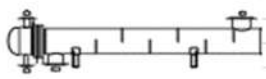

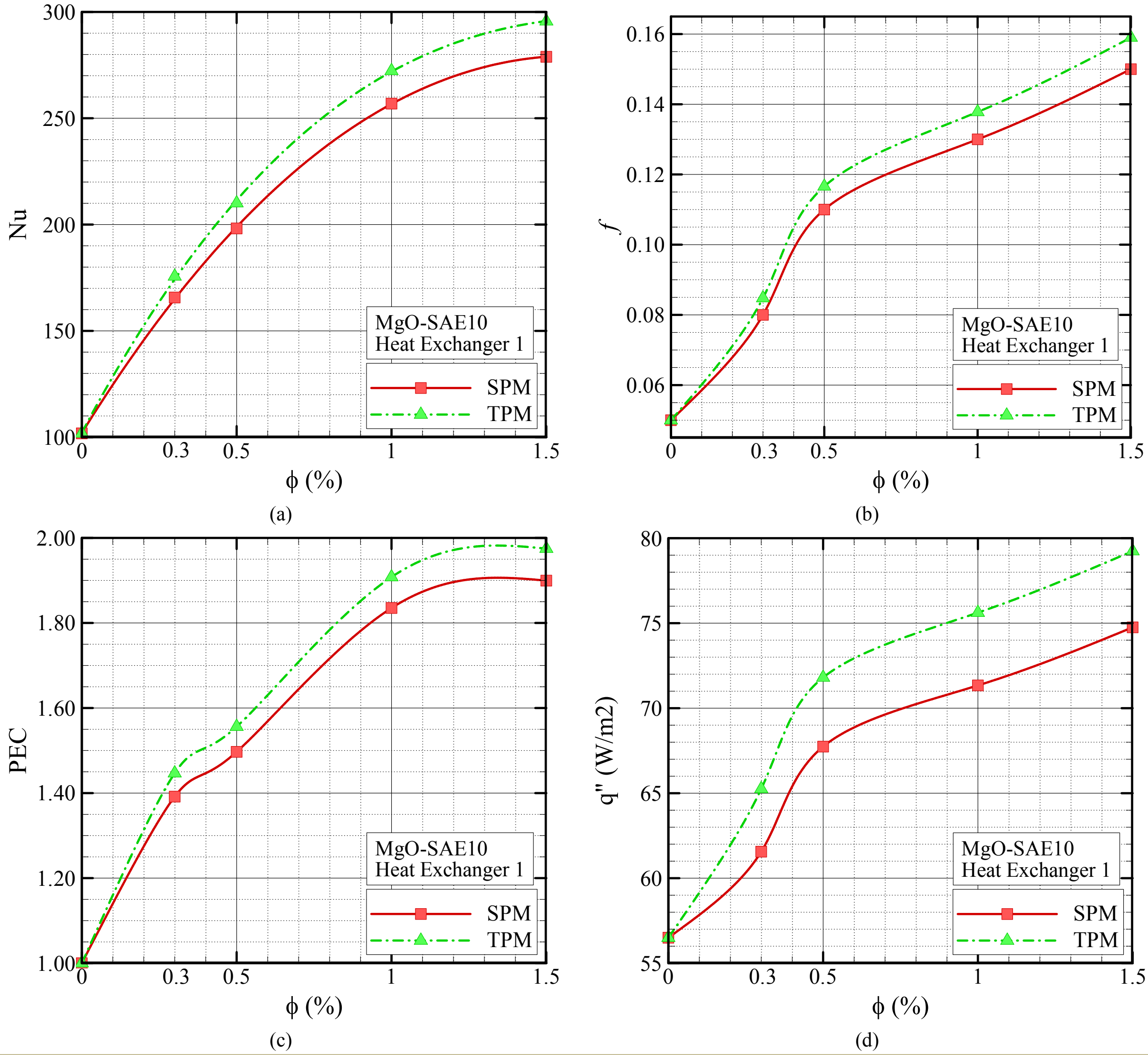

Fig. 10: Comparison of results for different phase models simulations in case of (a) average Nusselt number, (b) friction factor, (c) Thermal-Hydraulic Performance Evaluation Criteria and (d) specific heat transfer, versus different nanoparticles volume concentrations for Heat Exchanger number 1 filled with MgO-SAE10 nanofluid

3.2.2. Usage of Turbulators

Fig. 12 illustrates the comparison of results of models with different fins thickness using TPM simulations in case of average Nusselt number, friction factor, Thermal-Hydraulic Performance Evaluation Criteria, and specific heat transfer with different nanopaticles volume concentrations for Heat Exchanger number 1 (l=4.4mm and D=4.4mm) filled with MgO-SAE10 nanofluid. As it is seen in Fig. 12a, the usage of turbulators has a significant influence on the improvement of thermal characteristics and increases the Nusselt number value about 46%. Also, it is realized that the changing of fins thickness can affect the heat transfer performances. The usage of fins with δ=0.5mm leads to a higher Nusselt number in all ranges of studied volume fractions, and it is followed by the models with δ=0.8mm and δ=0.2mm respectively. It is clear that the fin with more thickness has more heat transfer surface area. However, it should be noted that it also leads to less fluid flow. Therefore, the usage of fin with δ=0.5mm has better thermal characteristics than the model with δ=0.8mm. As it is presented in Fig. 12b, with an increase in the thickness of fins, the friction factor also increases. Further thickness leads to higher turbulence and destroys the laminar sub-layers; it finally leads to further pressure drop from the inlet to the outlet. Therefore the configuration with δ=0.2mm has the minimum friction factor values and is followed by δ=0.5mm and δ=0.8mmrespectively.

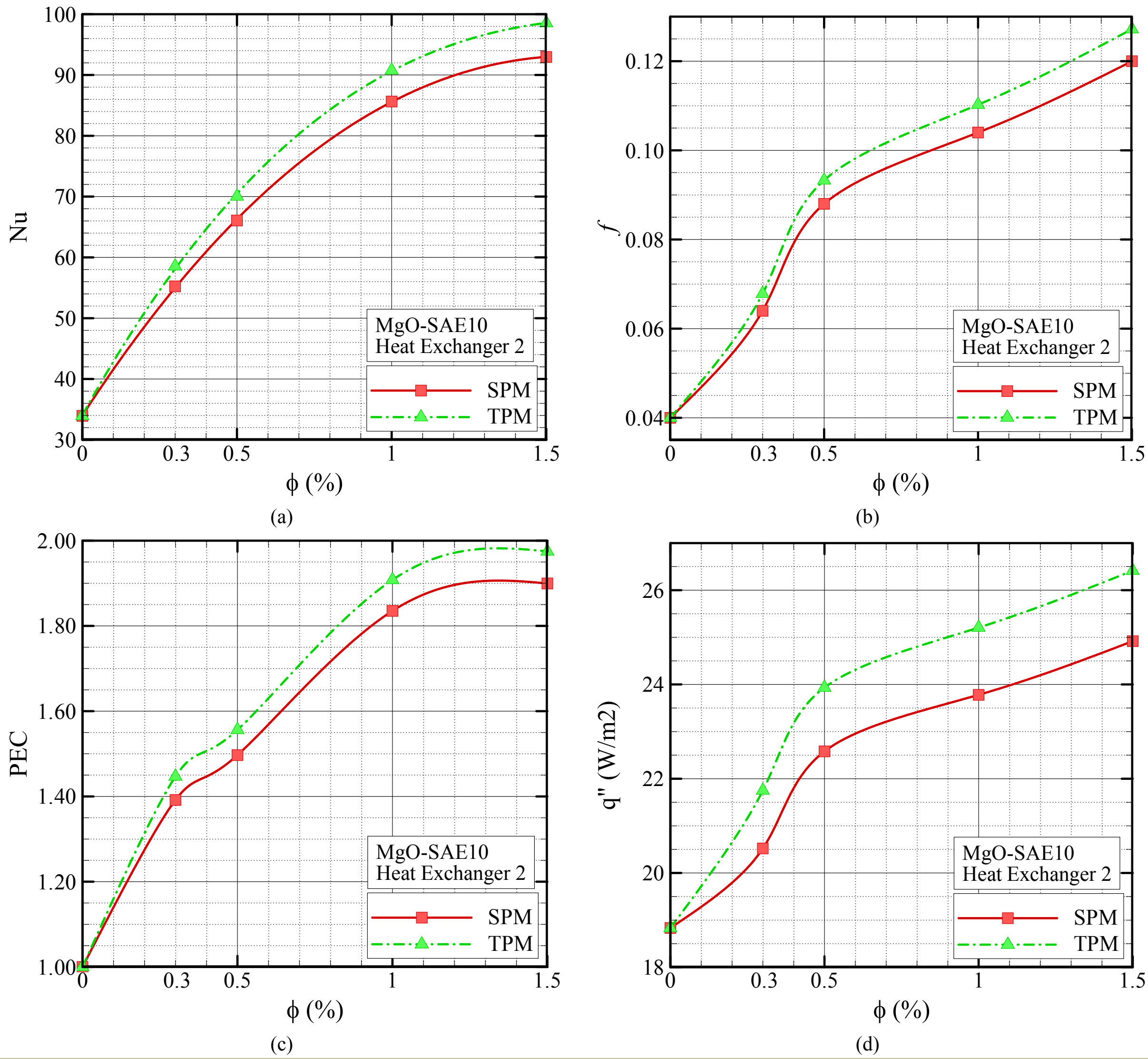

Fig. 11: Comparison of results for different phase models simulations in case of (a) average Nusselt number, (b) friction factor, (c) Thermal-Hydraulic Performance Evaluation Criteria and (d) specific heat transfer, versus different nanoparticles volume concentrations for Heat Exchanger number 2 filled with MgO-SAE10 nanofluid

Furthermore, it is seen that the usage of turbulators increases the friction factor values significantly, and the friction factor values always increase by an increase in nanopaticles volume fractions. Fig. 12c demonstrates that the model with maximum Nusselt number values (δ=0.5mm) has the maximum THPEC values, and the model with δ=0.2mm (the minimum friction factor value) is not at the first stage. The best THPEC value is followed with δ=0.8mm and δ=0.2mm respectively. Also, it is seen that the usage of turbulators increases the THPEC values significantly, and the THPEC values always increase by an increase in nanopaticles volume fractions. Therefore, it is seen that higher Nusselt number values overcome the factors of less friction. Fig. 12d illustrates that heat flux changes have similar behaviors with THPEC variations and the configuration with δ=0.5mm has the maximum q'' values in ranges of all studied nanopaticles volume fractions, which is followed with models with δ=0.8mm and δ=0.2mm respectively. Furthermore, it is seen that the usage of turbulators increase heat flux values significantly, and the heat flux values always increase by an increasing in nanopaticles volume fractions.

Therefore, the configuration with δ=0.5mm is adopted as the best thickness value for Heat Exchanger number 1 and is used in the rest of this study to analyze other geometrical parameters of turbulators.

Fig. 13 illustrates the comparison of results of models with different fins thickness using TPM simulations in case of average Nusselt number, friction factor, Thermal-Hydraulic Performance Evaluation Criteria, and specific heat transfer, with different nanopaticles volume concentrations for Heat Exchanger number 2 (*l*=4.4mm and *D*=4.4mm) filled with MgO-SAE10 nanofluid. As it is seen in Fig. 13a, the usage of turbulators has a significant influence on the improvement of thermal characteristics and increases the Nusselt number value about 44%. Also, it is realized that the changing of fins thickness can affect the heat transfer performances. The usage of fins with δ=0.5mm leads to a higher Nusselt number in all ranges of studied volume fractions, and it is followed by models with δ=0.8mm and δ=0.2mm respectively.

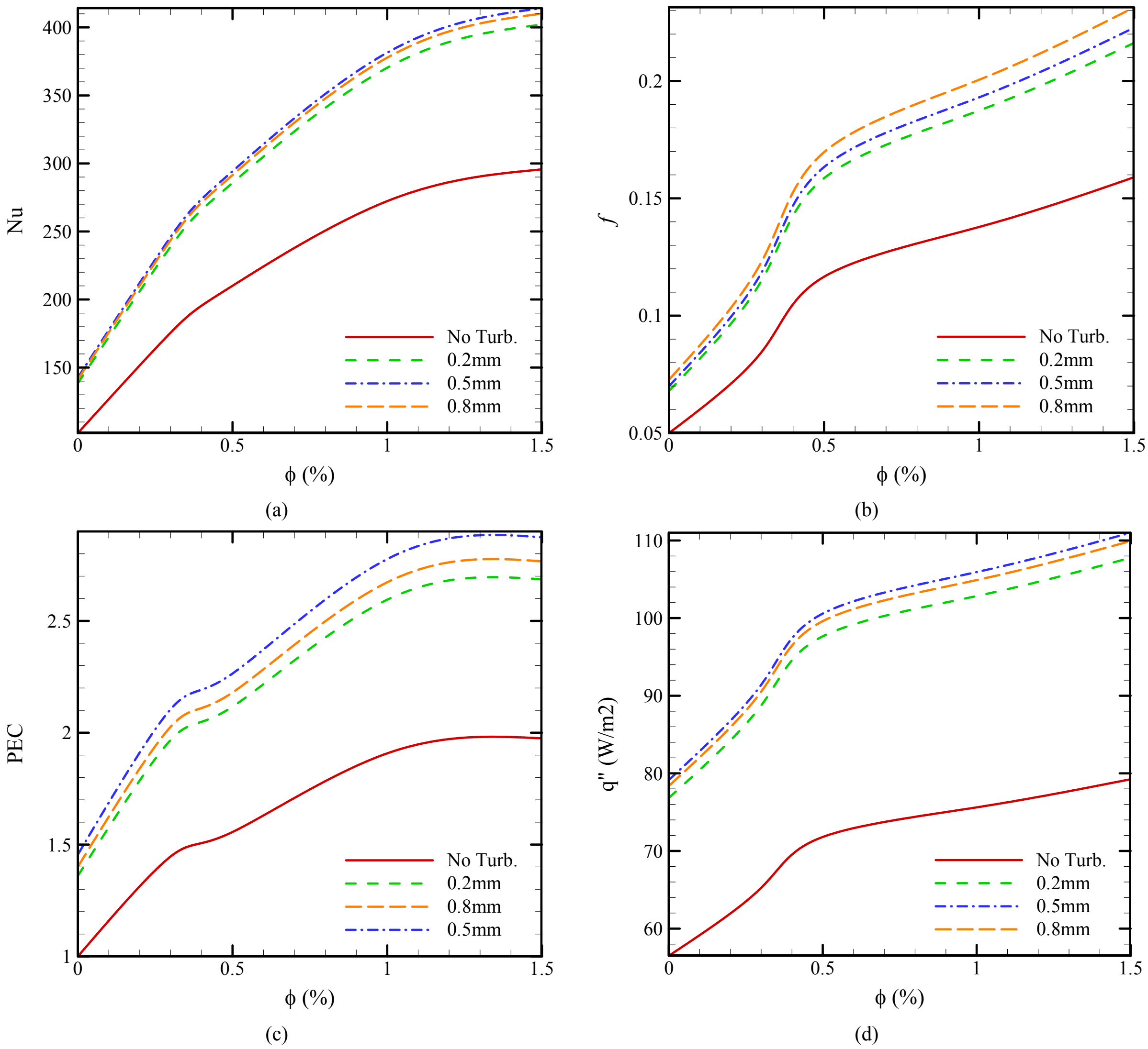

Fig. 12 Comparison of results for models with different fins thickness using TPM simulations in case of (a) average Nusselt number, (b) friction factor, (c) Thermal-Hydraulic Performance Evaluation Criteria and (d) specific heat transfer, versus different nanoparticles volume concentrations for Heat Exchanger number 1 (l=4.4mm and D=4.4mm) filled with MgO-SAE10 nanofluid

It is clear that the fin with more thickness has more heat transfer surface area. However, it should be noted that it leads also to less fluid flow. Therefore the usage of fin with δ=0.5mm has better thermal characteristics than the model with δ=0.8mm. As it is presented in Fig. 13b as the fins thickness increases, the friction factor also increases. More thickness leads to more turbulence and destroys the laminar sub-layers and finally lead to a more pressure drop from the inlet to the outlet. Therefore, the configuration with δ=0.2mm has the minimum friction factor values and is followed by δ=0.5mm and δ=0.8mmrespectively. Furthermore, it is seen that the usage of turbulators increases the friction factor values significantly and also the friction factor values always increase by an increase in nanopaticles volume fractions. Fig. 13c demonstrates that the model with maximum Nusselt number values (δ=0.5mm) has the maximum THPEC values, and the model with δ=0.2mm (the minimum friction factor value) is not at the first stage. The best THPEC value is followed with δ=0.8mm and δ=0.2mm respectively. Also, it is seen that the usage of turbulators increases the THPEC values significantly, and also the THPEC values always increase by an increase in nanopaticles volume fractions. Therefore, it is seen that a higher Nusselt number values overcome the less-friction factors.

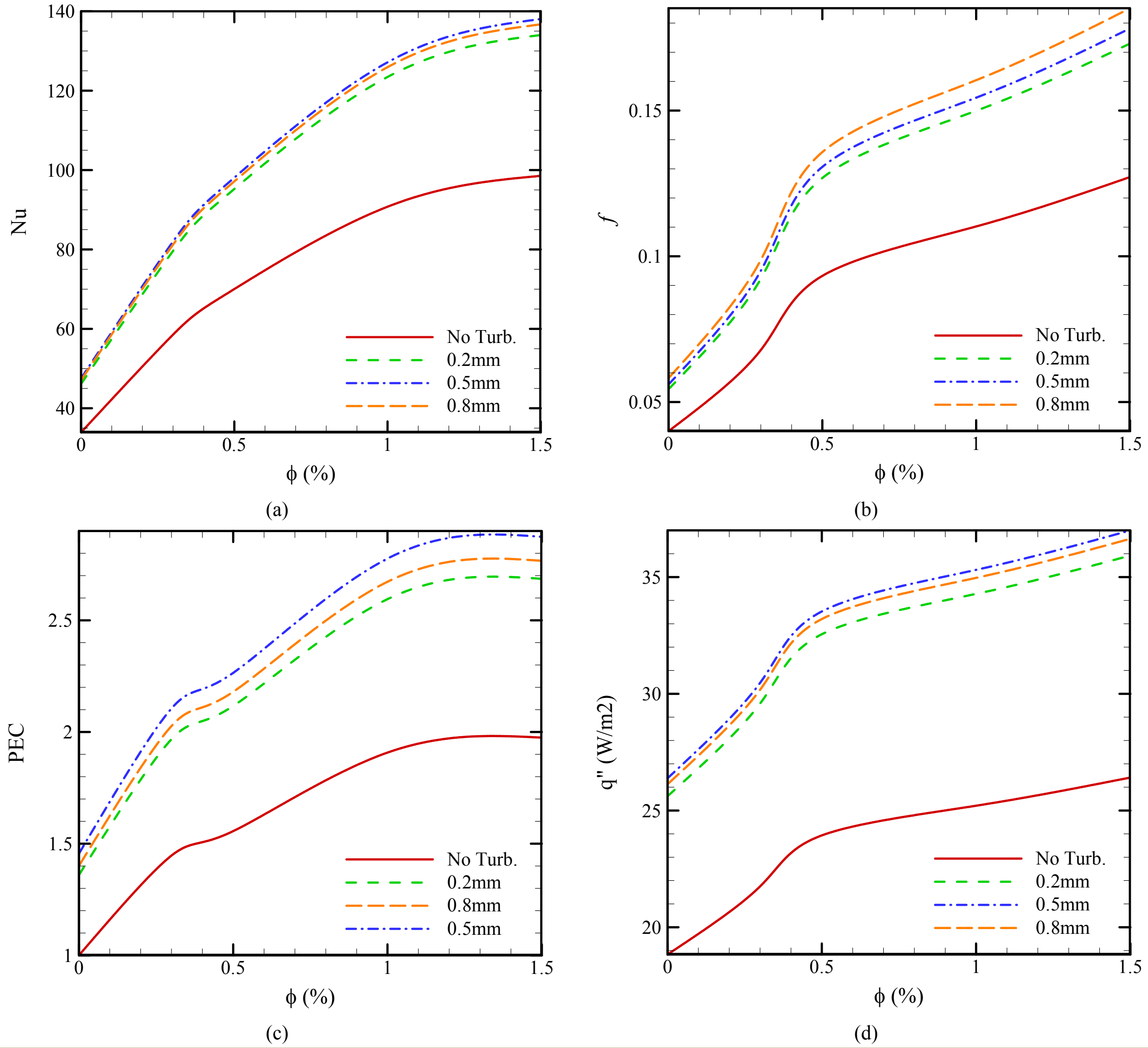

Fig. 13: Comparison of results for models with different fins thickness using TPM simulations in case of (a) average Nusselt number, (b) friction factor, (c) Thermal-Hydraulic Performance Evaluation Criteria and (d) specific heat transfer, versus different nanoparticles volume concentrations for Heat Exchanger number 2 (l=4.4mm and D=4.4mm) filled with MgO-SAE10 nanofluid

Fig. 13d illustrates that heat flux changes have a similar behavior with THPEC variations and the configuration with δ=0.5mm has the maximum q'' values in ranges of all studied nanopaticles volume fractions, which is followed with models with δ=0.8mm and δ=0.2mmrespectively. Furthermore, it is seen that the usage of turbulators increase the heat flux values significantly, and also the heat flux values always increase by by an increase in nanopaticles volume fractions.

Therefore the configuration with δ=0.5mm is adopted as the best thickness value for heat exchanger 2, and is used in the rest of this study to analyze other geometrical parameters of turbulators.

Fig. 14 demonstrates the comparison of results of models with different fins length using TPM simulations in case of average Nusselt number, friction factor, Thermal-Hydraulic Performance Evaluation Criteria, and specific heat transfer, with different nanopaticles volume concentrations for Heat Exchanger number 1 (δ=0.5mm and D=4.4mm) filled with MgO-SAE10 nanofluid. As it is seen in Fig. 14a, the change of fins lengths can affect the heat transfer performances. The usage of fins with l=5.8mm leads to a higher Nusselt number in all ranges of studied volume fractions, and it is followed by models with l=4.4mm and l=3.0mm respectively. It is clear that the fin with more length has more heat transfer surface area. Therefore, the usage of fin with l=5.8mm has better thermal characteristics than the model with l=4.4mm and l=3.0mm. As it is presented in Fig. 14b, with an increase in fin length, the friction factor also increases. Further thickness leads to further turbulence and destroys the laminar sub-layers. It finally leads to a more pressure drop from the inlet to the outlet. Therefore, the configuration with l=3.0mm has the minimum friction factor values and is followed by l=4.4mm and l=5.8mm respectively. Furthermore, it is seen that the friction factor values always increase by an increase in nanopaticles volume fractions. Fig. 14c demonstrates that the model with maximum Nusselt number and friction factor values (l=5.8mm) has the maximum THPEC values. The best THPEC value is followed with l=4.4mm and δ=3.0mm respectively. Also, it is seen that the THPEC values always increase by an increase in nanopaticles volume fractions. Therefore, it is seen that a higher Nusselt number values overcome the less-friction factors. Fig. 14d illustrates that heat flux changes have a similar behavior with THPEC variations and the configuration with l=5.8mm has the maximum q'' values in ranges of all studied nanopaticles volume fractions, which is followed with models with l=4.4mm and l=3.0mmrespectively. Furthermore, it is seen that the heat flux values always increase by an increase in nanopaticles volume fractions.

Therefore, the configuration with l=5.8mm is adopted as the best length value for Heat Exchanger number 1 and the configurations with δ=0.5mm and l=5.8mm are used in the rest of this study to analyze other geometrical parameters of turbulators.

Fig. 15 demonstrates the comparison of results of models with different fins length using TPM simulations in case of average Nusselt number, friction factor, Thermal-Hydraulic Performance Evaluation Criteria, and specific heat transfer, versus different nanoparticles volume concentrations for Heat Exchanger number 2 (δ=0.5mm and D=4.4mm) filled with MgO-SAE10 nanofluid. As it is seen in Fig. 15a, the change of fins lengths can affect heat transfer performances. The usage of fins with l=5.8mm leads to a higher Nusselt number in all ranges of studied volume fractions, and it is followed by models with l=4.4mm and l=3.0mmrespectively. It is clear that the fin with more length has more heat transfer surface area. Therefore, the usage of fin with l=5.8mm has better thermal characteristics than the model with l=4.4mm and l=3.0mm. As it is presented in Fig. 15b with an increase in fin length, the friction factor also increases. A further thickness leads to further turbulence and destroys the laminar sub-layers and finally leads to a more pressure drop from the inlet to the outlet. Therefore, the configuration with l=3.0mm has the minimum friction factor values and is followed by l=4.4mm and l=5.8mmrespectively. Furthermore, it is seen that the friction factor values always increase when nanoparticles volume fractions increase.

Fig. 15c demonstrates that the model with maximum Nusselt number and friction factor values (l=5.8mm) has the maximum THPEC values. The best THPEC value is followed with l=4.4mm and l=3.0mm respectively. Also, it is seen that THPEC values always increase by an increase in nanopaticles volume fractions. Therefore, it is seen that a higher Nusselt number values overcome the less friction factors. Fig. 15d illustrates that heat flux changes have similar behaviors with THPEC variations, and the configuration with l=5.8mm has the maximum q'' values in ranges of all studied nanopaticles volume fractions, which is followed by models with l=4.4mm and δ=3.0mm respectively. Furthermore, it is seen that the heat flux values always increase by an increase in nanopaticles volume fractions.

Therefore, the configuration with l=5.8mm is adopted as the best length value for heat exchanger 2, and configurations with δ=0.5mm and l=5.8mm are used in the rest of this study to analyze other geometrical parameters of turbulators.

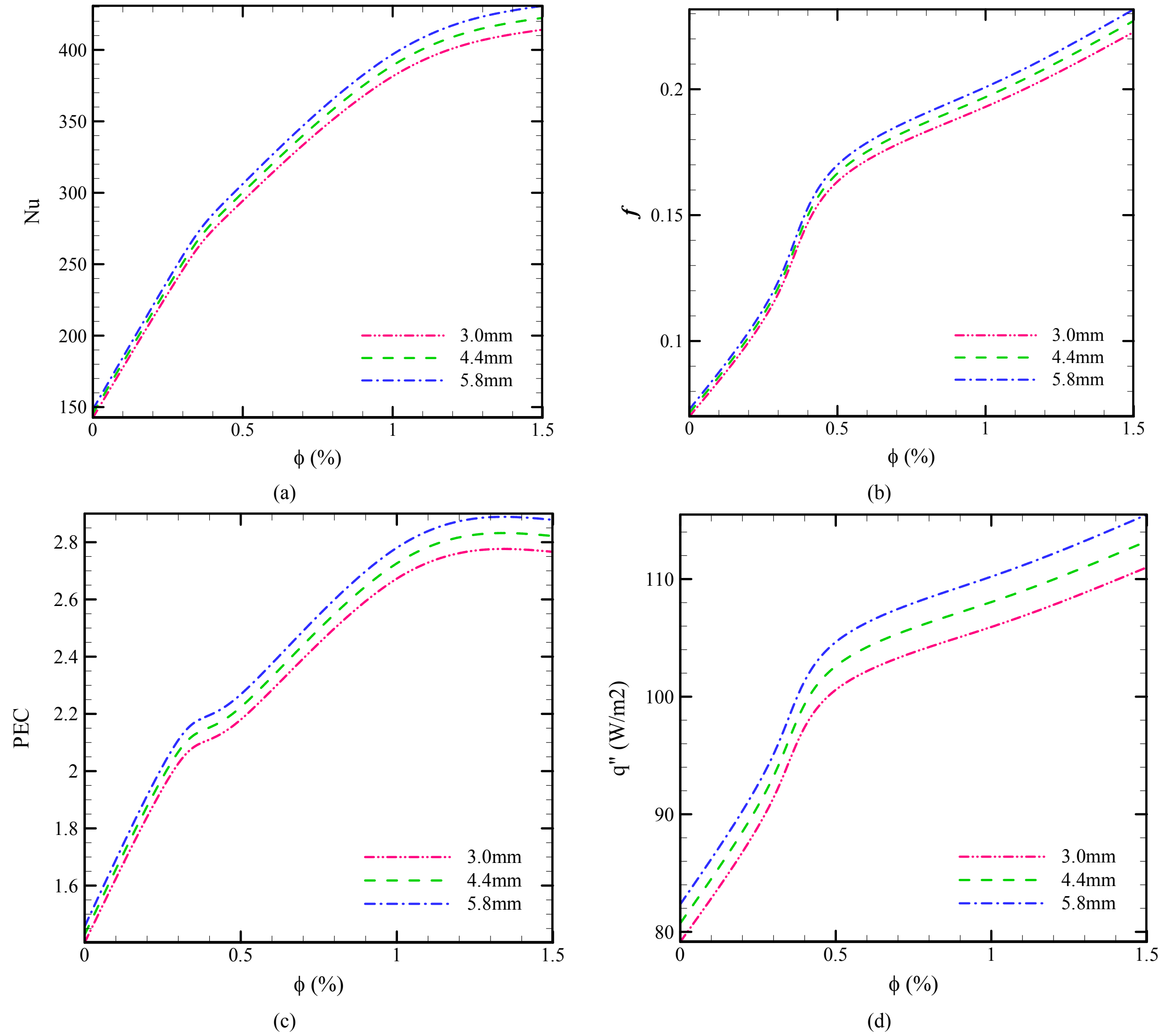

Fig. 14: Comparison of results for models with different fins length using TPM simulations in case of (a) average Nusselt number, (b) friction factor, (c) Thermal-Hydraulic Performance Evaluation Criteria and (d) specific heat transfer, versus different nanoparticles volume concentrations for Heat Exchanger number 1 (δ=0.5mm and *D*=4.4mm) filled with MgO-SAE10 nanofluid

Fig. 16 presents a comparison of results of models with different holes' diameters using TPM simulations in case of average Nusselt number, friction factor, Thermal-Hydraulic Performance Evaluation Criteria, and specific heat transfer, with different nanopaticles volume concentrations for Heat Exchanger number 1 (δ=0.5mm and *l*=5.8mm) filled with MgO-SAE10 nanofluid. As it is seen in Fig. 16a, the change of the diameters of the holes can affect the heat transfer performances. The usage of holes with *D*=5.8mm leads to a higher Nusselt number in all ranges of studied volume fractions, and it is followed by models with *D*=4.4mm and *D*=3.0mm respectively. It is clear that the holes with more diameters lead to more diffusions and, consequently, more heat transfer. Therefore, the usage of holes with *D*=5.8mm has better thermal characteristics than the models with *D*=4.4mm and *D*=3.0mm. As it is presented in Fig. 16b, with an increase in theholes' diameters, the friction factor reduces. Less diameters lead to more turbulence and destroy the laminar sub-layers and finally lead to more pressure drop from the inlet to the outlet. Therefore, the configuration with *D*=3.0mm has the minimum friction factor values and is followed by *D*=4.4mm and *D*=5.8mm respectively. Furthermore, it is seen that the friction factor values always increase by an increase in nanopaticles volume fractions. Fig. 16c demonstrates that the model with maximum Nusselt number and minimum friction factor values (*D*=5.8mm) has maximum THPEC values.

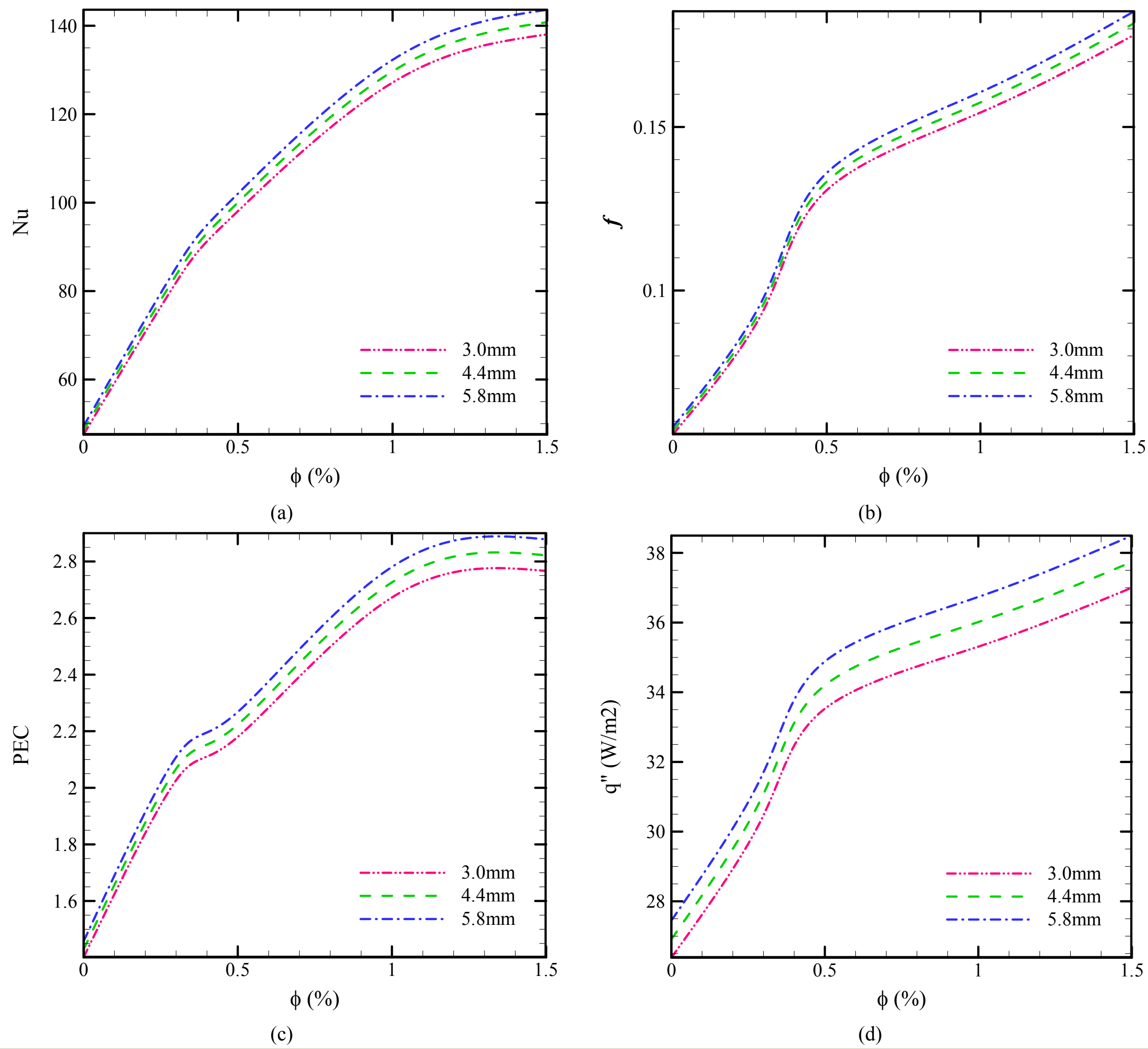

Fig. 15 Comparison of results for models with different fins length using TPM simulations in case of (a) average Nusselt number, (b) friction factor, (c) Thermal-Hydraulic Performance Evaluation Criteria and (d) specific heat transfer, versus different nanoparticles volume concentrations for Heat Exchanger number 2 (δ=0.5mm and D=4.4mm) filled with MgO-SAE10 nanofluid

The best THPEC value is followed by D=4.4mm and D=3.0mm respectively. Also, it is seen that THPEC values always increase by an increase in nanopaticles volume fractions. Fig. 16d illustrates that heat flux changes have similar behaviors with THPEC variations, and the configuration with D=5.8mm has the maximum q'' values in ranges of all studied nanopaticles volume fractions, which are followed by models with D=4.4mm and D=3.0mm respectively. Furthermore, it is seen that the heat flux values always increase by an increase in nanopaticles volume fractions.

Therefore, the configuration with D=5.8mm is adopted as the best hole diameter value for Heat Exchanger number 1 and δ=0.5mm,l=5.8mm, and D=5.8mm are introduced as the best geometrical parameters for Heat Exchanger number 1 in the present study.

Fig. 17 presents the comparison of results of models with different holes' diameters using TPM simulations in case of average Nusselt number, friction factor, Thermal-Hydraulic Performance Evaluation Criteria, and specific heat transfer, with different nanopaticles volume concentrations for Heat Exchanger number 2 (δ=0.5mm and l=5.8mm) filled with MgO-SAE10 nanofluid. As it is seen in Fig. 17a, the change of holes' diameters can affect the heat transfer performances. The usage of holes with D=5.8mm leads to a higher Nusselt number in all ranges of studied volume fractions, and it is followed by models with D=4.4mm and D=3.0mm respectively. It is clear that the holes with larger diameters lead to more diffusions and, consequently, more heat transfer. Therefore, the usage of holes with D=5.8mm has better thermal characteristics than the model with D=4.4mm and D=3.0mm. As it is presented in Fig. 17b, with an increase in the holes' diameters, the friction factor reduces. Smaller diameters lead to more turbulence and destroy the laminar sub-layers and finally lead to a more pressure drop from the inlet to the outlet. Therefore, the configuration with D=3.0mm has the minimum friction factor values and is followed by D=4.4mm and D=5.8mm respectively. Furthermore, it is seen that the friction factor values always increase by an increase in nanopaticles volume fractions. Fig. 17c demonstrates that the model with maximum Nusselt number and minimum friction factor values (D=5.8mm) has maximum THPEC values. The best THPEC value is followed by D=4.4mm and D=3.0mm respectively. Also, it is seen that THPEC values always increase by an increase in nanopaticles volume fractions. Fig. 17d illustrates that heat flux changes have similar behaviors with THPEC variations, and the configuration with D=5.8mm has the maximum q'' values in ranges of all studied nanoparticles volume fractions, which are followed by models with D=4.4mm and D=3.0mm respectively. Furthermore, it is seen that the heat flux values always increase by an increase in nanopaticles volume fractions.

Therefore, the configuration with D=5.8mm is adopted as the best hole diameter value for heat exchanger 2, and δ=0.5mm, l=5.8mm and D=5.8mm are introduced as the best geometrical parameters for heat exchanger 1 in the present study.

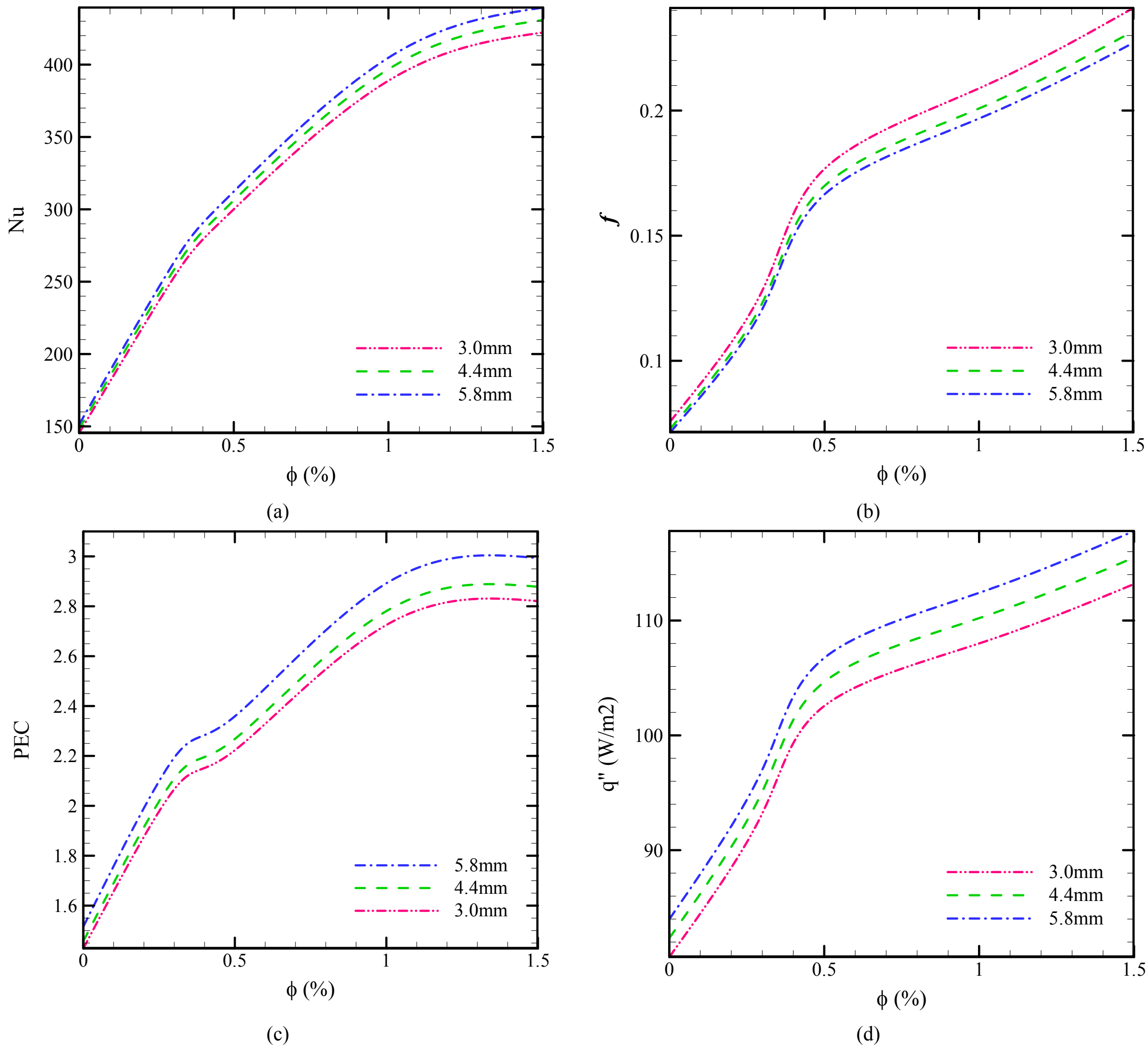

Fig. 16 Comparison of results for models with different holes diameters using TPM simulations in case of (a) average Nusselt number, (b) friction factor, (c) Thermal-Hydraulic Performance Evaluation Criteria and (d) specific heat transfer, versus different nanoparticles volume concentrations for Heat Exchanger number 1 (δ=0.5mm and l=5.8mm) filled with MgO-SAE10 nanofluid

3.3. Step Number Three

As it was seen in previous step, for both heat exchanger systems filled with MgO-SAE10 nanofluid, the usage of SOL-shaped turbulators with δ=0.5mm, l=5.8mm and D=5.8mm is suggested.

- The q'' and THPEC values for Heat Exchanger number 1, filled with MgO-SAE10 nanofluid, are 118.92 W/m^2 and 3.02respectively.
- The q'' and THPEC values for Heat Exchanger number 2, filled with MgO-SAE10 nanofluid, are 39.96 W/m^2 and 3.00 respectively.

Therefore, according to these new q'' values, novel heat exchangers are designed using Aspen-HYSYS software. Fig. 18 demonstrates a comparison between the reference and the novel Heat Exchangers, number 1 and 2, ingeometrical parameters in case of using MgO-SAE10 nanofluid. These figures clearly show that the usage of novel heat exchangers can sharply reduce the cost of manufacturing refinery heat exchangers.

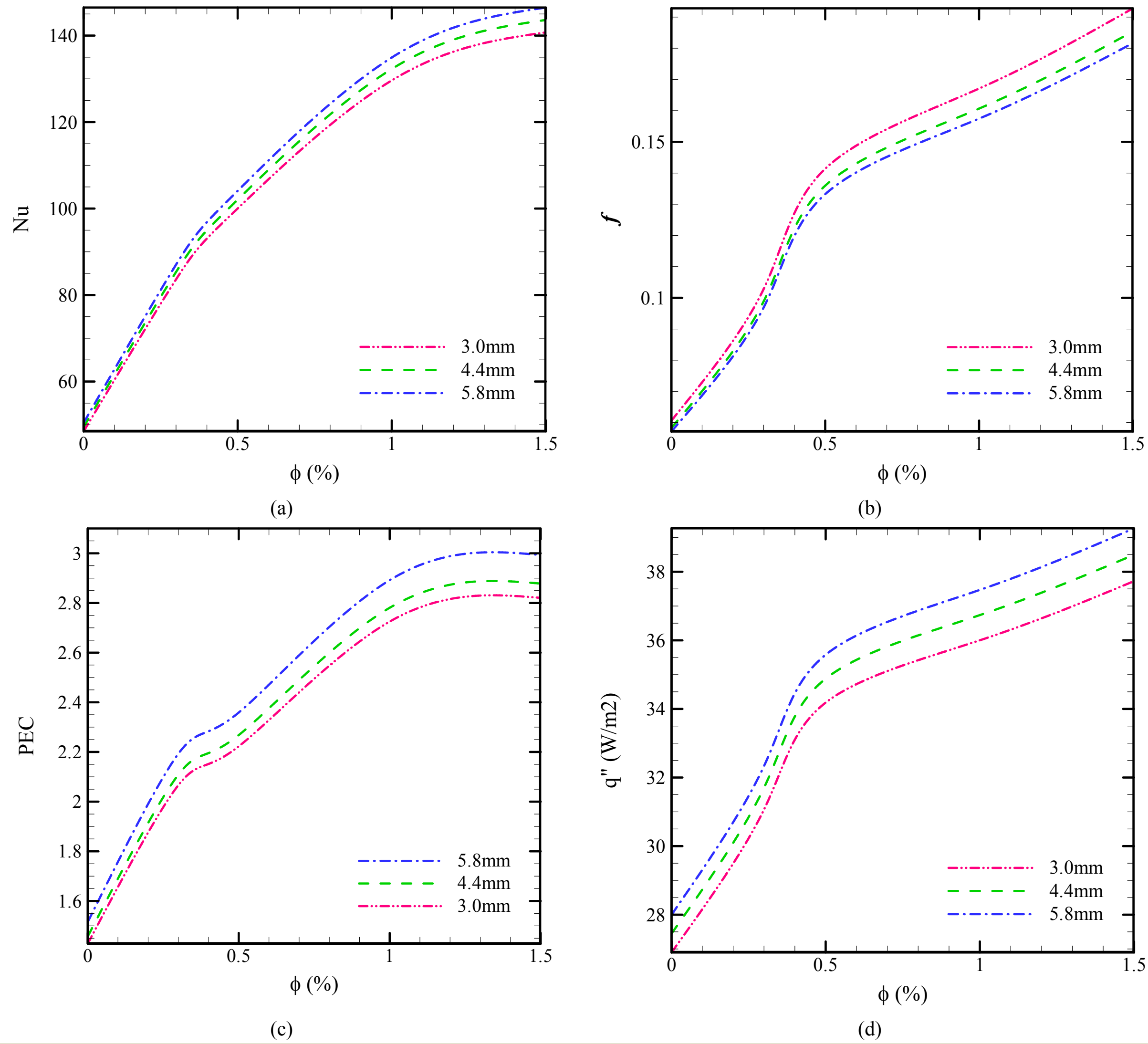

Fig. 17: Comparison of results for models with different holes diameters using TPM simulations in case of (a) average Nusselt number, (b) friction factor, (c) Thermal-Hydraulic Performance Evaluation Criteria and (d) specific heat transfer, versus different nanoparticles volume concentrations for Heat Exchanger number 2 (δ=0.5mm and l=5.8mm) filled with MgO-SAE10 nanofluid

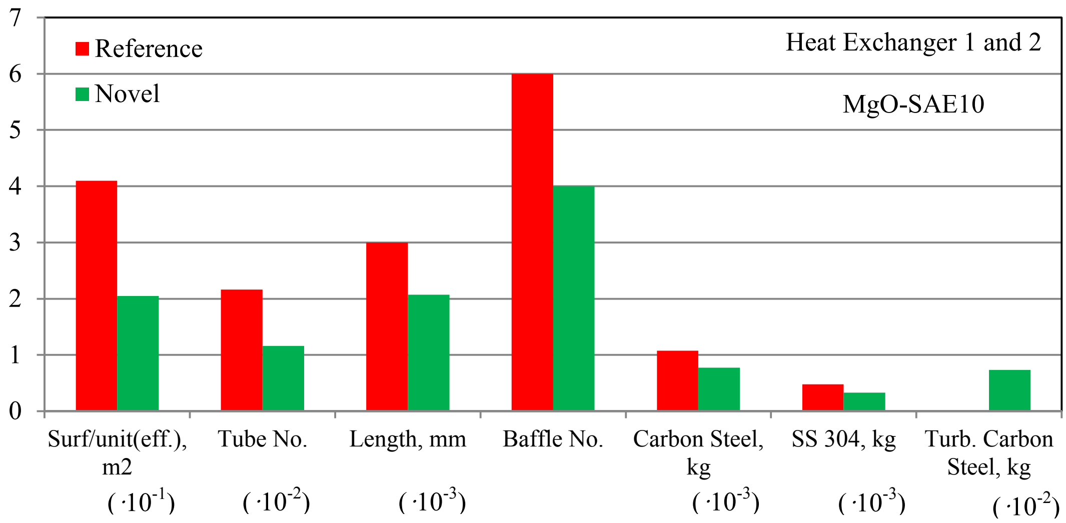

Fig. 18: Comparison between the reference and the novel Heat Exchangers number 1 and 2in geometrical parameters in case of using MgO-SAE10 nanofluid

4. Conclusion

A two-phase simulation of nanofluid flow in a heat exchanger equipped with vortex generator and the effects of different geometrical parameters of turbulators have been numerically investigated in the current investigation. The most important results which are obtained are as follow:

- The usage of nanofluid significantly increases the Nusselt number values, and at φ=1.5% the Nusselt number value can increase till about 174% and 190% than the base fluid for SPM and TPM respectively.
- Using nanofluid can increase the average friction factor till about 200% and 218% than the base fluid for SPM and TPM respectively.
- Employing nanofluid at all ranges of nanoparticles volume fractions is efficient according to a thermal-hydraulic viewpoint (THPEC > 1).
- The usage of turbulators in pipes has a significant effect on an average Nusselt number and increases the average Nusselt number sharply.
- Employing TPM simulation leads to a higher Nusselt number than using SPM for all studied turbulators.
- Changing fins thickness can affect heat transfer performances. The usage of fins with δ=0.5mm leads to a higher Nusselt number in all ranges of studied volume fractions, and it is followed by models with δ=0.8mm and δ=0.2mm respectively.
- The usage of fins with l=5.8mm leads to a higher Nusselt number in all ranges of studied volume fractions, and it is followed by models with l=4.4mm and l=3.0mm respectively.
- Changing the diameters of the holes' can affect the heat transfer performances. The usage of holes with D=5.8mm leads to a higher Nusselt number in all ranges of studied volume fractions, and it is followed by models with D=4.4mm and D=3.0mm respectively.
- The heat exchanger filled with MgO-SAE10 nanofluid and equipped with SOL-shaped turbulators with δ=0.5mm, l=5.8mm and D=5.8mm is suggested as the best configuration in this work.
- The q'' and THPEC values for Heat Exchanger number 1, filled with MgO-SAE10 nanofluid, are 118.92 W/m^2 and 3.02 respectively.
- The q'' and THPEC values for the Heat Exchanger number 2, filled with MgO-SAE10 nanofluid, are 39.96 W/m^2 and 3.00 respectively.

References

[1] Oyakawa, K. and Shinzato, T., I., "*The effects of the channel width on heat-transfer augmentation in a sinusoidal wave channel*", JSME International Journal, Vol. 32, pp. 403-410, 1989.

[2] Panahi, D. and Zamzamian, K., "*Heat transfer enhancement of shell-and-coiled tube heat exchanger utilizing helical wire turbulator*", Applied Thermal Engineering, Vol. 115, pp. 607-615, 2017.

[3] Feyza Akyürek, E., Geliş, K., Şahin, B. and Manay, E., "*Experimental analysis for heat transfer of nanofluid with wire coil turbulators in a concentric tube heat exchanger*", Results in Physics, Vol. 9, pp. 376-389, 2018.

[4] Ničeno, B., Nobile, E. "*Numerical analysis of fluid flow and heat transfer in periodic wavy channels*", International Journal of Heat and Fluid Flow, Vol.4, No. 2, pp. 15-167, 2001.

[5] Sheikholeslami, M. and Ganji, D.D., "*Heat transfer improvement in a double pipe heat exchanger by means of perforated turbulators*", Energy Conversion and Management, Vol. 127, pp. 112-123, 2016.

[6] Comini, G., Nonino, C. and Savino, S., "*Effect of aspect ratio on convection enhancement in wavy channels*", Numerical Heat Transfer, Part A: Applications, Vol. 44, No. 1, pp. 21-37, 2003.

[7] Farshad, S. A. and Sheikholeslami, M., "*Numerical examination for entropy generation of turbulent nanomaterial flow using complex turbulator in a solar collector*", Physica A: Statistical Mechanics and its Applications, 2019.

[8] Liou, T.M.S., Chang, W. and Chan, S.P., "*Experimental study on thermal flow characteristics in square serpentine heat exchangers mounted with louver-type turbulators*", International Journal of Heat and Mass Transfer, Vol. 116, pp. 897-908, 2018.

[9] Rivier, M., Sébastian, P., Guilhem, T. G. and Collignan, R. A., "*Heat transfer enhancement of a circular tube heat exchanger fitted with an elliptic shaped turbulator designed in the context of developing countries*", Applied Thermal Engineering, Vol. 81, pp. 92-101, 2015.

[10] Jafaryar, M., Sheikholeslami, M. and Li, Z., "*CuO-water nanofluid flow and heat transfer in a heat exchanger tube with twisted tape turbulator*", Powder Technology, Vol. 336, pp. 131-143, 2018.

[11] Duan, Z. and Muzychka, Y.S., "*Effects of axial corrugated roughness on low Reynolds number slip flow and continuum flow in microtubes*", Journal of Heat Transfer, Vol. 132, No. 4, pp. 1-8, 2010.

[12] Zhang, L. and Che, D., "*Influence of corrugation profile on the thermal hydraulic performance of cross-corrugated plates*", Numerical Heat Transfer, Part A: Applications, Vol. 59, No. 4, pp. 267-296, 2011.

[13] Zhang, L. and Che, D., "*Turbulence models for fluid flow and heat transfer between cross-corrugated plates, Numerical Heat Transfer*", Part A: Applications, Vol. 60, No. 5, pp. 410-440, 2011.

[14] Santra, A.K., Sen, S. and Charaborty, N., "*Study of heat transfer due to laminar flow of copper–water nanofluid through two isothermally heated parallel plates*", International Journal of Thermal Sciences, Vol. 48, No. 2, pp.391-400, 2009.

[15] Abu-Nada, E., "*Application of nanofluids for heat transfer enhancement of separated flows encountered in a backward facing step*", International Journal of Heat and Fluid Flow, Vol. 29, No. 1, pp. 242–249, 2008.

[16] Xiong, Q., Jafaryar, M., Divsalar, A., Sheikholeslami, M., Shafee, A. and Dat D. Vo, "*Muhammad Humran Khan, I. Tlili, Zhixiong Li, Macroscopic simulation of nanofluid turbulent flow due to compound turbulator in a pipe*", Chemical Physics, Vol. 527, 2019.

[17] Xiong, Q., yani, A., Azeez, M., Barzinjy, A., Nasir Dara, R., Shafee, A. and Nguyen-Thoi, T., "*Modeling of heat transfer augmentation due to complex-shaped turbulator using nanofluid*", Physica A: Statistical Mechanics and its Applications, Vol. 540, 2020.

[18] Manca, O., Nardini, S. and Ricci, D., "*A numerical study of nanofluid forced convection in ribbed channels*", Applied Thermal Engineering, Vol. 37, pp. 280-292, 2012.

[19] Mohammed, H.A., Al-Shamani, A.N. and Sheriff, J.M., "*Thermal and hydraulic characteristics of turbulent nanofluids flow in a rib-groove channel*", International Communications in Heat and Mass Transfer, Vol. 39, No. 10, pp. 1584-1594, 2012.

[20] Heidary, H. and Kermani, M.J., "*Effect of nanopaticles on forced convection in sinusoidal-wall channel*", International Communications in Heat and Mass Transfer, Vol. 37, No. 10, pp. 1520-1527, 2010.

[21] Sheikholeslami, M., Gorji-Bandpy, M. and Ganji, D.D., "*Effect of discontinuous helical turbulators on heat transfer characteristics of double pipe water to air heat exchanger*", Energy Conversion and Management, Vol. 118, pp. 75-87, 2016.

[22] Ahmed, M.A., Shuaib, N.H. and Yusoff, M.Z., "*Numerical investigations on the heat transfer enhancement in a wavy channel using nanofluid*", International Journal of Heat and Fluid Flow, Vol.55, No. 21-22,pp. 5891-1598, 2012.

[23] Ahmed, M.A., Shuaib, N.H. and Yusoff, M.Z., "*Effects of geometrical parameters on the flow and heat transfer characteristics in trapezoidal-corrugated channelusing nanofluid*", International Communications in Heat and Mass Transfer, Vol.42, pp. 69-74, 2013.

[24] Abbasian Arani, A.A., Sodripour, S. and Kermani, S., "*Nanoparticle shape effects on thermal-hydraulic performance of boehmite alumina nanofluids in a sinusoidal–wavy mini-channel with phase shift and variable wavelength*", International Journal of Mechanical Sciences, Vol. 128–129, pp. 550-563, 2017.

[25] Sodripour, S., Ghorashi, S.A. and Estajloo, M., "*Numerical Investigation of a Cavity Equipped with Corrugated Heat Source: A Full Convection-Conduction-Radiation Coupling*", American Journal of Aerospace Engineering, Vol. 4, No. 3, pp. 27-37, 2017.

[26] Sheikholeslami, M. and Ganji, D.D., "*Heat transfer enhancement in an air to water heat exchanger with discontinuous helical turbulators; experimental and*

numerical studies", Energy, Vol. 116, pp. 341-352, 2016.

[27] Sandeep P. Nalavade, Chandrakant L. Prabhune, "*Narayan K. Sane, Effect of novel flow divider type turbulators on fluid flow and heat transfer*", Thermal Science and Engineering Progress, Vol. 9, pp. 322-331, 2019.

[28] Mashoofi, N., Pesteei, S. M., Moosavi, A. and Sadighi Dizaji, H., "*Fabrication method and thermal-frictional behavior of a tube-in-tube helically coiled heat exchanger which contains turbulator*", Applied Thermal Engineering, Vol. 111, pp. 1008-1015, 2017.

[29] Yadav, S. and Sahu, S. K., "*Heat transfer augmentation in double pipe water to air counter flow heat exchanger with helical surface disc turbulators*", Chemical Engineering and Processing - Process Intensification, Vol. 135, pp. 120-132, 2019.

[30] Nanan, K., Thianpong, C., Pimsarn, M., Chuwattanakul, V. and Eiamsa-ard, S., "*Flow and thermal mechanisms in a heat exchanger tube inserted with twisted cross-baffle turbulators*", Applied Thermal Engineering, Vol. 114, pp. 130-147, 2017.

[31] Zeinali Heris, S., Etemad, S.Gh. and Esfahany, N.M., "*Numerical investigation of nanofluid laminar convective heat transfer through a circular tube*", Numerical Heat Transfer, Part A: Applications, Vol. 52, No. 11, pp. 1043-1058, 2007.

[32] Mohammed, H.A., Abuobeidab, I.A.M.A., Vuthaluru, H.B. and Liua, S., "*Two-phase forced convection of nanofluids flow in circular tubes using convergent and divergent conical rings inserts*", International Communications in Heat and Mass Transfer, Vol. 101, pp. 10–20, 2019.

[33] Karimi, A., Al-Rashed, A.A.A., Afrand, M., Mahian, O., Wongwises, S. and Shahsavar, A., "*The effects of tape insert material on the flow and heat transfer in a nanofluid-based double tube heat exchanger: Two-phase mixture model*", International Journal of Mechanical Sciences, Vol. 156, pp. 397-409, 2019.

[34] Sheikholeslami, M. and Rokni, H.B., "*Influence of melting surface on MHD nanofluid flow by means of two phase model*", Chinese Journal of Physics, 2018.

[35] Sheikholeslami, M. and Rokni, "*Nanofluid two phase model analysis in existence of induced magnetic field*", International Journal of Heat and Mass Transfer, Vol. 107, pp. 288–299, 2017.

[36] Alsarraf, J., Moradikazerouni, A., Shahsavar, A., Afrand, M., Salehipour, H. and Tran, M.D., "*Hydrothermal analysis of turbulent boehmite alumina nanofluid flow with different nanoparticle shapes in a minichannel heat exchanger using two-phase mixture model*", Physica A, 2019.

[37] Borah, A., Boruah, M.P. and Pati, S., "*Conjugate heat transfer in a duct using nanofluid by two-phase Eulerian–Lagrangian method: Effect of non-uniform heating*", Powder Technology, 2019.

[38] Barnoon, P., Toghraie, D., Eslami, F. and Mehmandoust, B., "*Entropy generation analysis of different nanofluid flows in the space between two concentric horizontal pipes in the presence of magnetic field: Single-phase and two-phase approaches*", Computers and Mathematics with Applications, 2019.

[39] Asadi, A. and Pourfattah, F., "*Heat transfer performance of two oil-based nanofluids containing ZnO and MgO nanoparticles; a comparative experimental investigation*", Powder Technology, Vol. 343, pp. 296-308, 2019.

[40] Patankar, S.V., "Numerical Heat Transfer and Fluid Flow", Taylor & Francis Group, 1980.

[41] Sodripour, S., "*3D Numerical Analysis of Atmospheric-Aerosol/Carbon-Black Nanofluid Flow within a Solar Air Heater Located in Shiraz*", Iran, International Journal of Numerical Methods for Heat and Fluid Flow, Vol. 29, No. 4, pp. 1378–1402, 2019.

[42] Sodripour, S. and Chamkha, A.J., "*The Effect of Nanoparticle Morphology on Heat Transfer and Entropy Generation of Supported Nanofluids in a Heat Sink Solar Collector*", Thermal Science and Engineering Progress, Vol. 9, pp. 266–280, 2019.

[43] Sodripour, S., "*Investigation of Flow Characteristics and Heat Transfer Enhancement of a Corrugated Duct using Nanofluid*", Journal of Applied Mechanics and Technical Physics, Vol. 59, No. 6, pp. 1049–1057, 2018.

[44] Sodripour, S., "*First and Second Laws Analysis and Optimization of a Solar Absorber; Using Insulator Mixers and MWCNTs Nanoparticles*", Global Journal of Researches in Engineering A: Mechanical and Mechanics, Vol. 17, No. 5, pp. 37–48, 2017.

[45] Sodripour, S., Adibi, M. and Sheikhzadeh, G.A., "*Two Different Viewpoints about using Aerosol-Carbon Nanofluid in Corrugated Solar Collectors: Thermal-Hydraulic Performance and Heating Performance*", Global Journal of Researches in Engineering A: Mechanical and Mechanics, Vol. 17, No. 5, pp. 19–36, 2017.

[46] Corcione, M., "*Empirical correlating equations for predicting the effective thermal conductivity and dynamic viscosity of nanofluids*", Energy Conversion and Management, Vol. 52, pp. 789-793, 2011.

[47] Keblinski, P., Phillpot, S.R., Choi, S.U.S. and Eastman, J.A., "*Mechanisms of heat flow in suspensions of nanosized particles (nanofluids)*", International Journal of Heat and Mass Transfer, Vol. 45, pp. 855–63, 2002.

[48] Launder, B.E. and Spalding, D.B., "*Mathematical Models of Turbulence*", Academic Press, New York, 1972.

[49] Anderson, J.D., "*Computational Fluid Dynamics*", McGraw-Hill, New York, 1995.

[50] Kim, D., Kwon, Y., Cho, Y., Li, C., Cheong, S., Hwang, Y., Lee, J., Hong, D. and Moon, S., "*Convective heat transfer characteristics of nanofluids under laminar and turbulent flow conditions*", Current Applied Physics, Vol. 9, No. 2, pp. 119-123, 2009.

[51] Anvari, A.R., Javaherdeh, K., Emami-Meibodi, M. and Rashidi, A.M., "*Numerical and experimental investigation of heat transfer behavior in a round tube with the special conical ring inserts*", Energy Conversion and Management, Vol. 88, pp. 214–217, 2014.

[52] Promvonge, P. and Eiamsaard, S., "*Heat transfer behaviors in a tube with combined conical-ring and twisted-tape insert*", International Communications in Heat and Mass Transfer, Vol. 34, pp. 849–859, 2007.